World Journal of Gastroenterology

Submit a Manuscript: https://www.f6publishing.com

World J Gastroenterol 2023 September 28; 29(36): 5180-5197

DOI: 10.3748/wjg.v29.i36.5180

ISSN 1007-9327 (print) ISSN 2219-2840 (online)

REVIEW

Liver metastases: The role of magnetic resonance imaging

Cesare Maino, Federica Vernuccio, Roberto Cannella, Francesco Cortese, Paolo Niccolò Franco, Clara Gaetani, Valentina Giannini, Riccardo Inchingolo, Davide Ippolito, Arianna Defeudis, Giulia Pilato, Davide Tore, Riccardo Faletti, Marco Gatti

Specialty type: Gastroenterology and hepatology

Provenance and peer review: Invited article; Externally peer reviewed.

Peer-review model: Single blind

Peer-review report's scientific quality classification

Grade A (Excellent): 0
Grade B (Very good): 0
Grade C (Good): C, C
Grade D (Fair): 0
Grade E (Poor): 0

P-Reviewer: Xiao B, China; Zhang H, China

Received: July 30, 2023
Peer-review started: July 30, 2023
First decision: August 15, 2023
Revised: August 28, 2023
Accepted: September 11, 2023
Article in press: September 11, 2023
Published online: September 28, 2023

Cesare Maino, Paolo Niccolò Franco, Davide Ippolito, Department of Radiology, Fondazione IRCCS San Gerardo dei Tintori, Monza 20900, Italy

Federica Vernuccio, University Hospital of Padova, Institute of Radiology, Padova 35128, Italy

Roberto Cannella, Giulia Pilato, Department of Biomedicine, Neuroscience and Advanced Diagnostics (BiND), University of Palermo, Palermo 90127, Italy

Francesco Cortese, Riccardo Inchingolo, Unit of Interventional Radiology, F Miulli Hospital, Acquaviva delle Fonti 70021, Italy

Clara Gaetani, Valentina Giannini, Arianna Defeudis, Davide Tore, Riccardo Faletti, Marco Gatti, Department of Surgical Sciences, University of Turin, Turin 10126, Italy

Davide Ippolito, School of Medicine, University of Milano Bicocca, Milano 20100, Italy

Corresponding author: Marco Gatti, MD, Assistant Professor, Doctor, Department of Surgical Sciences, University of Turin, Via Genova 3, Turin 10126, Italy. marcogatti17@gmail.com

Abstract

The liver is one of the organs most commonly involved in metastatic disease, especially due to its unique vascularization. It's well known that liver metastases represent the most common hepatic malignant tumors. From a practical point of view, it's of utmost importance to evaluate the presence of liver metastases when staging oncologic patients, to select the best treatment possible, and finally to predict the overall prognosis. In the past few years, imaging techniques have gained a central role in identifying liver metastases, thanks to ultrasonography, contrast-enhanced computed tomography (CT), and magnetic resonance imaging (MRI). All these techniques, especially CT and MRI, can be considered the non-invasive reference standard techniques for the assessment of liver involvement by metastases. On the other hand, the liver can be affected by different focal lesions, sometimes benign, and sometimes malignant. On these bases, radiologists should face the differential diagnosis between benign and secondary lesions to correctly allocate patients to the best management. Considering the above-mentioned principles, it's extremely important to underline and refresh the broad spectrum of liver metastases features that can occur in everyday clinical practice. This review aims to summarize the most common imaging features of liver metastases, with a special focus on typical and atypical appearance, by using MRI.

Key Words: Liver metastases; Magnetic resonance imaging; Gadolinium; Gd-EOB-DTPA; Gadoxetate disodium; Liver specific contrast agents; Hepatobiliary contrast agents

Core Tip: To better detect liver metastases, magnetic resonance imaging (MRI) protocol should be correctly performed, using extra-cellular or hepatobiliary contrast agents. Even if conventional non-enhanced techniques can help depict focal liver lesions, contras-enhanced sequences are mandatory, to evaluate their behavior in comparison to the healthy liver parenchyma. These aspects allow to determine liver and hepatic lesions' vascularization over time and increase radiologists' diagnostic values. The typical appearance of liver metastases can be easily recognized as hypovascular lesions. However, some primary tumors can produce liver metastases with atypical appearances, such as hypervascular ones, or within calcification, mucin, or other proteins. The multiparametric nature of MRI, combined with the administration of contrast agents, can strongly increase radiologists' confidence in the final diagnosis.

Citation: Maino C, Vernuccio F, Cannella R, Cortese F, Franco PN, Gaetani C, Giannini V, Inchingolo R, Ippolito D, Defeudis A, Pilato G, Tore D, Faletti R, Gatti M. Liver metastases: The role of magnetic resonance imaging. *World J Gastroenterol* 2023; 29(36): 5180-5197
URL: https://www.wjgnet.com/1007-9327/full/v29/i36/5180.htm
DOI: https://dx.doi.org/10.3748/wjg.v29.i36.5180

INTRODUCTION

The liver is one of the most common sites of metastatic disease, accounting for up to 25% of all secondary lesions to solid organs due to its unique architectural and vascular composition that provides fertile soil for different primary neoplasms to spread. Consequently, metastases represent the most frequent malignant liver tumors, being about 18-40 times more frequent than primary hepatic neoplasms[1]. Cancers from the gastrointestinal tract, breast, lung, pancreas, neuroendocrine tumors, and melanomas commonly spread to the liver[2,3]. Specifically, colorectal cancers (CRCs) are widespread, as 50% of such patients presenting with metastatic liver disease at diagnosis or during the follow-up after surgery[4].

Metastatic spread to the liver represents one of the major prognostic factors, determining the clinical outcome[5,6]. Surgical resection is considered the treatment option with the best curative potential for liver metastases. In the case of unresectable disease, besides systemic chemotherapy, many liver-directed approaches have been developed, including local therapies, such as stereotactic body radiation therapy or radiofrequency ablation, and regional therapies, like peptide receptor radionuclide therapy, hepatic artery directed infusional chemotherapy, trans-arterial chemoembolization and trans-arterial radioembolization (TARE)[7]. Hence, accurate detection and assessment of secondary liver lesions are pivotal to select the most tailored management approach for each patient and to determine in whom an improved overall survival rate may be expected.

Magnetic resonance imaging (MRI) represents the reference standard radiological technique for the detection of liver metastases, with its higher sensitivity and specificity compared to computed tomography (CT) and fluoro-2-deoxyglucose positron emission tomography (FDG-PET)[8,9]. The evaluation of secondary liver lesions is one of the most common clinical indications for liver MRI in radiologists' daily practice.

On these bases, the aim of this review is to summarize the role of MRI in the detection and assessment of liver metastases, describing their main imaging features and focusing on the added value of the most recent imaging tools.

MAGNETIC RESONANCE PROTOCOLS

A comprehensive MRI protocol for liver metastases detection and follow-up after systemic, surgical or locoregional treatments should include the acquisition of T1- and T2W (T1W and T2W) sequences, diffusion weighted imaging (DWI) sequences, dynamic multiphase and/or delayed sequence after intravenous administration of gadolinium-based contrast agents (GBCAs). GBCAs, with intravascular-interstitial distribution, are generally used with T1W sequences, with or without fat suppression techniques. Dynamic contrast enhanced acquisitions improve the identification and characterization of liver metastases depending on their enhancement behavior[10].

The introduction of hepatocyte-specific GBCAs, notably Gd-BOPTA (gadobenate dimeglumine-MultiHance®, Bracco) and Gd-EOB-DTPA (Gadoxetic acid, disodium-Primovis®/Eovist®, Bayer), has increased more and more MRI sensibility and specificity for liver metastases imaging. These GBCAs are taken up by hepatocytes and excreted in the biliary system and they are extremely valuable in follow-up after locoregional or systemic treatments. These molecules present a biphasic enhancement pattern; the first phase, immediately after intravenous injection, is similar to CT dynamic enhancement after iodine contrast injection while a delayed phase occurs after 10 to 120 min after injection[10,11]. Lesions

not containing hepatocytes cannot take up such molecules; therefore, metastasis appear hypointense compared with surrounding healthy liver parenchyma[12].

Super paramagnetic iron oxide (SPIO) iron-based nanoparticles contrast media were withdrawn from the market in western countries even if they are still used in clinical practice in some oriental countries such as Japan; the target of this class of contrast agents are reticuloendothelial cells (RES)[10].

In clinical practice, MRI liver protocols must be adapted to the patient's specific clinical questions and characteristics [13].

It is recommended to acquire slices as thin as possible (*i.e.* 3-5 mm), with rectangular field of view (FOV) appropriated to the habitus of the patient. Acquisition plans must include at least axial and coronal. Matrices may vary depending on the sequences used; they should be as high as possible bearing in mind contrast-to-noise ratio. A higher spatial and contrast resolution may be obtained employing 2D and 3D T1W sequences. Temporal resolution is related to the length of acquisition time of a single MRI scan, according to patient's compliance[10].

With modern MRI scanners, the possibility to acquire multiple arterial phases allows either to improve spatial resolution or to reduce scanning time, which is important in case of patients with limited breath-hold capacity or in pediatric ones[10,11].

Non-contrast acquisition

Gradient-echo T1 in-phase and out-of-phase: Gradient-echo (GRE) sequences are prone to susceptibility and chemical shift artifacts and such property may be used to detect and quantify iron and fat deposition within liver parenchyma or in focal lesions[14]. Chemical shift artifacts are due to the lower precession frequency of fat protons compared to water ones [15]. Such differences result in periodic phase coherence (in-phase), where every voxel signal is the sum of water and fat signal or opposition (out-of-phase) of water and fat signals, whereas the two signals have a phase difference of 180°, and thus nulling each other out[16]. Such sequences permit the detection of intracellular fat, either in hepatic lesions or in the hepatic parenchyma[14,16].

Fast spin-echo or turbo spin-echo T2 sequences, with or without fat-suppression: They are very rapid sequences; at present also acquired by breath-hold technique. They are characterized by a 90° excitation pulse followed by a train of several 180° refocusing pulses to fill several K-space lines (echo train) during a repetition time. Fluid content is the predominant information obtained from this kind of sequences, thus allowing to discriminate between solid and cystic-like focal lesions. Fat-suppression should be regularly used to increase contrast resolution[16].

Diffusion-weighted imaging: They are basically T2W images, acquired with single shot, echo-planar imaging (EPI) technique and fat-suppression. They are crucial to rapidly acquire the diffusion signal before it nulls[10,17]. Different series of diffusion-weighted images are obtained by modifying the gradient strength and magnitude (b-value). One series must be acquired with a b-value of 0, so that no gradient is applied and consequently no diffusion information is present, providing similar information as T2 fat-sat sequences. Other series must be acquired with increasing b-values (b50, b400, b800)[18]. These are fundamental for secondary lesion detection, as there is a "black-blood" effect, which increases conspicuity of lesions located next to the vessels. Series acquired with a high b-value (b800) are essential for liver lesion characterization: Highly cellular tissues, such as metastases, present restriction to diffusion thus appearing hyperintense in DWI images[17,18]. EPI sequences are prone to motion artifacts: Breath-hold scans have the advantage of reduced blurring and ghosting artifacts, however their short acquisition times limit spatial resolution, the number of excitations, and number of possible b-values[17,18]. On the other hand, navigator or respiratory-triggered techniques improve image signal-to-noise ratio (SNR) at higher b-values, reducing motion artifacts and blurring[14].

Post-contrast acquisition

Dynamic evaluation: GRE 2D or 3D T1 sequences with or without fat-suppression, acquired before and after GBCA administration[19]. T1W sequences are very sensitive to susceptibility artifacts thus enabling to detect iron, calcium, air or metal[16]. 3D sequences are being used more and more frequently, they are acquired with a modified Dixon technique, that explores the chemical shift effect of fat and water, allowing to separate fat and water peaks allowing to improve the homogeneity of the images, fat-suppression, and providing thinner slice thickness and slice overlap[16]. GRE 3D T1W fat-sat sequences (LAVA, VIBE, THRIVE, *etc.*) are the classical sequences used for dynamic contrast-enhanced studies to evaluate the vascularization pattern of the lesion, usually acquiring one dynamic phase for each breath-hold, about every 25-30 s[19].

At present time, some techniques (CAIPIRINHA, TWIST-VIBE, DISCO or THRIVE 4D sequences, *etc.*), based on parallel imaging and compressed sensing, allow to obtain multi-arterial acquisition in one breath-hold[20]. Non-Cartesian acquisition schemes, for example radial sampling, may be performed for dynamic studies jointly with compressed sensing and parallel imaging, further increasing temporal resolution permitting free-breathing dynamic evaluation (Siemens GRASP VIBE sequences), with reduced motion artifacts, in a sort of continuous acquisition[19,20].

Hepatobiliary-reticuloendothelial phases are T1W sequences, with or without fat-sat, if Gd-BOPTA or Gd-EOB-DTPA, both increasing T1 relaxivity, have been administered[12,19]. Proton density or T2W sequences are used with SPIOs contrast agents[12,19]. For Gd-BOPTA, hepatobiliary phase (HBP) imaging is recommended after 90-120 min, thus requiring the patient to return to the scanner for final T1W imaging of the liver and bile ducts[11,12]. For Gd-EOB-DTPA, HBP acquisition may be performed after 20 min, while the patient is still on the scanner[5,12]. On HBP there is an increase in signal intensity of the hepatic normal parenchyma compared to a non-hepatocytic lesion, thus improving Magnetic resonance (MR) sensibility in detection and characterization of different types of liver lesion[5,10,12]. Furthermore, increasing the flip angle of a T1W 3D sequence from 10° to 30° (Siemens scanner 1.5 T) in the HBP, visually and quantit-

atively improves the visualization of the biliary ducts, obtaining high quality hepatobiliary images[21].

Additional sequences: Half-Fourier Acquisition Single-shot Turbo spin Echo (HASTE), heavily T2W, with a rapid acquisition time, and acquired *via* breath-hold technique. They are used mainly to evaluate lesions or structures with prominent fluid content: They are the basic sequences for the evaluation of biliary tree and pancreatic ducts (MR colangiopancreatography)[22].

Balanced steady-state GRE (true FISP, FIESTA, balanced fast field echo). They tend to highlight fluid content providing a highly accurate morphologic imaging as well as a good delineation of vessels and ductal structures. Furthermore, due to their extremely rapid acquisition time (200 ms), these sequences can tolerate optimally motion artifacts.

Other additional sequences might be added on a case-by-case basis (sequences for fat and iron overload quantification) [8,9,11].

EXTRA-CELLULAR AND HEPATOBILIARY CONTRAST AGENTS: HOW, WHEN, AND WHY?

Contrast-enhanced sequences are mandatory to correctly characterize focal liver abnormalities to assess the vascular behavior of liver parenchyma and lesions.

Extra-cellular contrast agents (ECAs) have historically represented the reference standard for liver-enhanced MRI. All ECAs are distributed within the extra-cellular interstitial space, and despite manufacturers or chemical formulations, they shorten T1 relaxation time, producing a signal intensity enhancement during their biodistribution. From a practical point of view, enhancement proprieties are similar to iodinated contrast media for CT, firstly with the opacification of hepatic arteries and hypervascular lesions (arterial phase, 30-40 s after bolus administration), then liver parenchyma and portal vein (portal-venous phase, 60-80 s after bolus administration), and finally by moving into the interstitial space (delayed phase, 180-300 s after bolus administration). After whole-body distribution, the excretion is entirely through the kidneys [23].

More recently, the introduction of hepatobiliary contrast agents (HBAs) added relevant information to the previous clinical practice, showing some degree of biliary excretion. Due to their ability to bind specific receptors regularly expressed in healthy hepatocytes [organic anion transporter (OATP)], HBAs allow the acquisition of the so-called HBP and consequently can increase the diagnostic accuracy for different focal liver lesions. In fact, after the administration of contrast medium bolus, the initial biodistribution is similar to those of ECAs, providing multi-phase dynamic post-contrast imaging. Moreover, after a specific time, healthy hepatocytes start the uptake of HBAs, which will then be excreted into the biliary ducts. Consequently, in the HBP images, both the liver and the biliary tree are significantly enhanced, while liver vessel and non-hepatocellular lesions show a low signal intensity[24].

Only two HBAs are approved for the clinical practice: Gd-BOPTA and Gd-EOB-DTPA[25]. When using Gd-BOPTA, about 3%-5% of the contrast dose is eliminated by biliary excretion. In contrast, with Gd-EOB-DTPA, about half of the dose is taken up by hepatocytes and excreted with the bile. Thus, these two contrast media need different acquisition times to obtain diagnostic HBP images, which are acquired about 1.5-3 h after Gd-BOPTA injection and about 15-20 min after Gd-EOB-DTPA administration in non-cirrhotic livers. Consequently, the HBP can be acquired at the end of the liver MRI protocol in the case of Gd-EOB-DTPA, while in a second step in the case of Gd-BOPTA[26,27]. Figure 1 summarizes MRI protocols by using ECAs and HBAs.

Choosing the best contrast media when acquiring a liver MR protocol cannot be straightforward, considering that both ECAs and HBAs present advantages and disadvantages. It's well-known that arterial phase acquisition during ECAs' administration can be more robust in comparison with Gd-EOB-DTPA because the latter leads to a lower enhancement of healthy parenchyma (reducing the lesion to liver contrast) and the higher frequency of artifacts[28]. Moreover, ECAs allow better detection of lesion washout over time, while the rapid uptake of Gd-EOB-DTPA precludes its evaluation during the transitional phase (acquired 180'' to 300'' after injection).

On the other hand, the evaluation of HBP can increase contrast resolution between liver parenchyma and secondary lesions. Mainly, one of the most relevant advantages of HBAs is the easy detection of non-hepatocellular lesions and lesions with non-functioning hepatocytes, including hepatic adenomas, hepatocellular carcinoma (HCC), and metastases. Indeed, when impaired hepatocytes are present, the whole lesion or part of it can be easily depictable as hypointense during the HBP images. Moreover, HBAs can increase diagnostic accuracy in the case of focal nodular hyperplasia (FNH), where functioning hepatocytes increase the uptake of contrast agents, resulting in a hyperintense lesion during the HBP [29].

Due to the high specificity and sensitivity in detecting hepatic focal lesions, HBAs should always be preferred in oncologic patients with known extra-hepatic primary cancer, especially in cases of increased risk of the disease's spread to the liver. The number and location of liver secondary lesions can significantly modify the patient's management and is crucial for treatment strategies' success[30].

Considering that patients with known primary tumors should undergo different follow-up examinations, abbreviated MRI (AMRI) protocols-composed of DWI, T2W, and HBP - have been proposed. In a recently published review, the Authors summarize the advantages and disadvantages of these new approaches. Even if not recommended nor approved by either international society, AMRI could increase the availability of MRI examinations and therefore facilitate strict surveillance of liver metastases, preserving an acceptable accuracy in their detection and characterization[31].

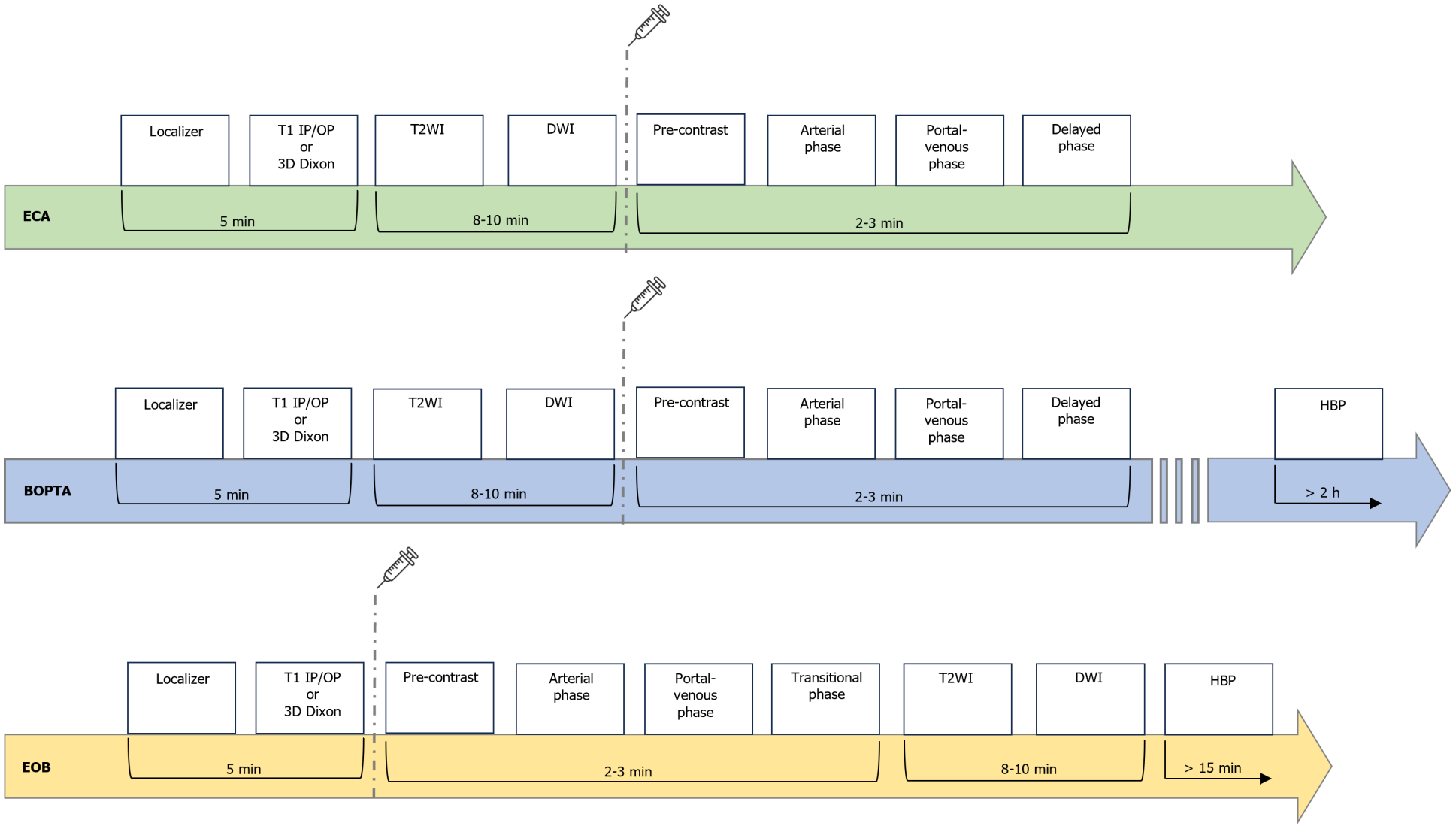

DOI: 10.3748/wjg.v29.i36.5180

Figure 1 Schematic summary of magnetic resonance imaging protocols by using ECAs and hepatobiliary contrast agents (Gd-BOPTA and Gd-EOB-DTPA). ECA: Extra-cellular; BOPTA: Gadobenate dimeglumine; EOB: Gadoxetic acid, disodium; T1 IP: T1-weighted in-phase imaging; T1 OP: T1-weighted out-of-phase imaging; DWI: Diffusion weighted imaging; HBP: Hepatobiliary phase; T2WI: T2-weighted imaging; HBP: Hepatobiliary phase.

CONVENTIONAL MRI FEATURES OF LIVER METASTASES

Typical appearance

Liver metastases typically occur as multifocal nodular lesions but less frequently they can occur as a solitary lesion, large confluent masses, or have an infiltrative appearance with multiple small lesions spread in the hepatic parenchyma (Figure 2). Two other rare patterns of distribution include the miliary diffusion which can be observed in lung, breast carcinomas, uveal melanoma, and neuroendocrine tumors and metastases situated in the gallbladder fossa in gallbladder cancer due to peculiar venous drainage[32]. Liver metastases from extrahepatic carcinomas usually have ill-defined margins and can present variable sizes, ranging from small nodules to bulky masses. MRI sequences like DWI and HBP images are particularly useful to identify small lesions, especially those with diameters < 1 cm[33].

The typical appearance of liver metastases is variable depending on the primary cancer, the lesions size, the extent of the disease, and background liver tissue (Figure 3). On non-contrast MRI, liver metastases are classically hypointense compared to the surrounding liver parenchyma. A slightly hypointense rim can be observed at the periphery of the lesions, reflecting the most viable tissue. Radiologists should be aware that some metastases can demonstrate various degrees of spontaneous hyperintensity on T1W images, suggesting the presence of high protein concentration (mucinous tumors), necrosis (colorectal adenocarcinomas), melanin (melanoma) or methemoglobin (hemorrhage)[34]. Fat in mass is not observed in hepatic metastases with few exceptions on fat-containing tumors such as liposarcomas or malignant teratomas[35,36]. On T2W images, liver metastases can demonstrate variable mild to moderate T2 hyperintensity, reflecting the variable amount of hypercellularity and internal desmoplastic fibrotic stroma. Elevated signal on T2W images is related to cystic or necrotic changes in larger metastatic lesions, whereas smaller lesions may appear isointense. Marked hyperintensity on T2W sequences may be detected in metastases from neuroendocrine tumors, which can resemble the imaging appearance of small hemangiomas. Up to 25% of liver metastases can demonstrate a targetoid appearance on T2W images, also known as target sign, which is characterized by a mild central T2 hyperintensity surrounded by a peripheral rim of moderate-to-marked T2 hyperintensity[32]. DWI and the apparent diffusion coefficient (ADC) map are useful to detect liver metastases, showing a restricted diffusion with ADC values lower than those of the parenchyma because of increased cellularity of the lesions. Targetoid appearance can be observed also on DWI, with a peripheral rim of marked diffusion restriction indicating the peripheral proliferative area of the metastases as opposed to the central necrotic region[37].

On post-contrast images, liver metastases can be classified according to the enhancement pattern on the late hepatic arterial phase as hypovascular or hypervascular metastases, as detailed below. On the portal-venous phase, hepatic metastases show washout, either complete or more prominent at the lesion's periphery. The peripheral washout sign, in which a peripheral rim is hypointense compared to the lesion's center and to surrounding parenchyma, can be present in both hypervascular and hypovascular metastases, but it's observed more frequently in hypervascular ones[38]. Histopathologically, peripheral washout might reflect perfusion alterations at the peripheral area of the lesions, which presents good arterial supply and good venous drainage of contrast[37]. It is important to note that washout appearance should be assessed on portal-venous and delayed phases when using ECAs, while it can be evaluated exclusively on portal-venous phase when Gd-EOB-DTPA is administered, as its uptake by functional hepatocytes starts at approximately 90 s after the contrast injection[39].

Liver metastases are typically hypointense compared to the background liver tissue on the HBP acquired after the administration of HBAs. However, metastases can also demonstrate a targetoid appearance on the HBP with marked hypointensity at the periphery of the lesion as opposed to the central cloud of enhancement likely due to contrast accumulation in the extracellular space or central fibrotic stroma[40,41]. Aberrant expression of OATP transporters has also been occasionally reported in CRC liver metastases[42]. Compared to FDG-PET and CT, EOB-MRI demonstrated the highest sensitivity (93.1%) in detecting liver secondary lesions with improved specificity (87.3%) in comparison with CT [43]. Moreover, MRI can significantly improve liver metastases detection in patients with hepatic steatosis, which can be easily overlooked on CT especially when small in size[44].

Hypovascular metastases

Hypovascular metastases are lesions in which the arterial phase enhancement is inferior or similar compared to that of the healthy liver and therefore appear hypointense on the late hepatic arterial phase. Arterial phase hypoenhancement is the most frequent pattern in liver metastases and it can be typically observed in gastrointestinal carcinomas, bladder, prostate, and lung cancers. These lesions typically demonstrate persistent hypoenhancement on the post-arterial phases and are hypointense on the HBP (Figure 4).

Hypervascular metastases

Hypervascular metastases manifest as lesions in which the arterial phase enhancement is higher compared to that of the liver parenchyma and therefore appear as hyperintense on the late hepatic arterial phase. The arterial phase hyperenhancement can be heterogenous and it can be observed in the whole or part of the lesions or be more pronounced at the periphery (*e.g.* rim arterial phase hyperenhancement). Hypervascular liver metastases with whole lesion hyperenhancement typically arise from hypervascular primary cancers such as neuroendocrine ones, renal cancer, melanoma, and thyroid cancer. These lesions can demonstrate early wash-out on the portal-venous phase or, more rarely, fading or persistent enhancement on post-arterial phases (Figures 5 and 6).

Metastases with peripheral arterial phase hyperenhancement are characterized by a targetoid appearance on post-contrast phases, showing rim hyperenhancement on arterial phase with washout on portal-venous or delayed phases, reflecting the increased cellularity at the lesion's periphery, in comparison with the central hypo-perfused area[37,45].

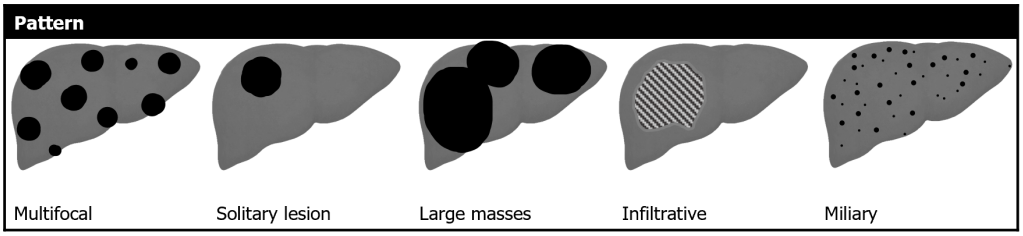

DOI: 10.3748/wjg.v29.i36.5180

Figure 2 Schematic representation of morphological liver metastases appearance.

MRI can improve the detection of arterial phase hyperenhancement by acquiring multiple arterial phases. This technique allows to detect early enhancement that can be missed on late arterial phase with improvement in enhancement detection compared to single-phase acquisition[46,47]. However, its usefulness for differential diagnosis between liver metastases and other liver lesions needs to be validated. Finally, subtraction images should always be considered to detect the arterial phase hyperenhancement in lesions showing hyperintensity on pre-contrast T1W images.

Atypical appearance

In current clinical practice, unusual radiologic features of liver metastases may be found thus making it challenging to discriminate metastases from other focal liver lesions. Detailed knowledge of atypical imaging features of liver metastases with a good understanding of the histopathologic background is crucial for accurate differential diagnosis. Among these, metastases with cystic appearance, calcifications, or fat are herein discussed.

Cystic liver metastases: Cystic liver metastases usually appear on MRI as strongly hyperintense on T2W sequences, hypointense on non-contrast T1W images, with lack or rim enhancement on contrast-enhanced T1W images. They may occur mainly from CRC, pancreatic cancer, neuroendocrine tumors (NETs), ovarian cancer, gastrointestinal stromal tumors (GISTs), melanoma and sarcomas. The causative mechanisms of cystic appearance of liver metastases may vary [37,48]:

(1) Rapid growth beyond hepatic arterial blood supply of the lesion, thus causing central necrosis, such as in NETs, GISTs, sarcomas, melanomas, angiosarcomas, testicular carcinomas, or squamous cell carcinomas;

(2) Mucinous components of the primary tumor, such as in mucinous CRCs or ovarian carcinomas;

(3) Marked T2W hyperintensity due to the primary histological features;

And (4) Changes after chemotherapy, including necrosis or cystic or mucinous regression.

Mucinous metastases from CRC are particularly challenging in daily practice because, in addition to marked T2W hyperintensity, they show a lack of diffusion restriction in about 81% of cases, thus making the differential diagnosis with benign cysts very challenging[49].

Calcified liver metastases: Calcified liver metastases usually show small or diffuse calcifications appearing hypointense on both T1- and T2W imaging, and are better demonstrated on CT. Calcified liver metastases may occur mainly from CRC liver metastases, bone-forming tumors (osteosarcoma and chondrosarcoma), lung, breast, prostate, stomach, ovary, thyroid, neuroendocrine tumors, GISTs, neuroblastoma, and melanoma[50-52].

The causative mechanisms of the calcified appearance of liver metastases may vary:

(1) Dystrophic calcifications resulting from necrosis and/or hemorrhage within the tumor;

(2) Mucoid calcifications related to the presence of mucin produced by mucinous adenocarcinomas;

(3) Proper production due to the intrinsic nature of the primary metastasizing malignancies;

And (4) Changes after chemotherapy, including mineralization of necrotic tissue.

The occurrence of calcifications in CRC is well-known since the first years of the 1960s when Engel and Dockerty[53] described their occurrence in the primary tumor at pathology and Miele and Edmonds[54] identified them in liver metastases on abdominal radiographies in four patients, with pathology confirmation in three of the four patients. In patients with CRC, calcifications may be present in up to 11% of cases before chemotherapy[51] and in about 5% of cases after chemotherapy usually – though not always – indicating tumor response[55].

Fat-containing liver metastases: The occurrence of fat in liver metastases may be distinguished based on the fat distribution and type of fat into three different scenarios. First, intralesional macroscopic fat may be encountered in metastases from liposarcoma and will show hyperintensity on T2W non-fat-sat sequences, and heterogenous appearance on T1W images with moderate signal loss on opposed-phase and increased signal on in-phase images, indicating the presence of macroscopic fat. Second, intralesional intracellular fat may be encountered very rarely having been described in liver metastases from renal cancer[56]. Third, liver metastases from malignant teratomas can contain extracellular fat, calcifications, and necrotic components[35,36].

The role of MR in too small to characterize lesions

Too small to characterize (TSTC) liver lesions are defined as those small liver lesions - typically 1.5 cm in diameter or smaller - that cannot be confidently characterized on CT by the interpreting radiologist on the available images. In most cases, TSTCs are benign[57], and this is particularly true for solitary hepatic lesions up to 1 cm, that therefore do not

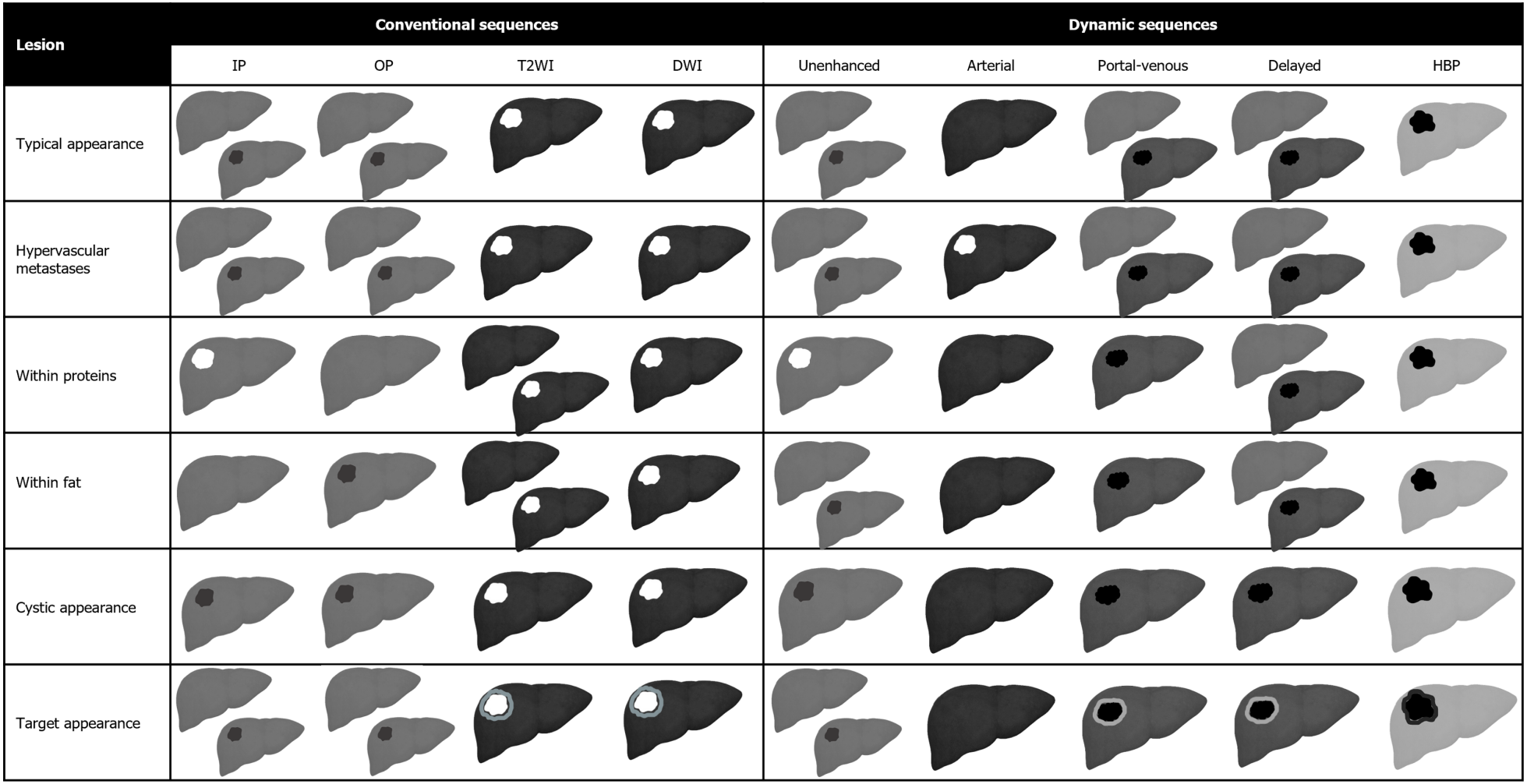

DOI: 10.3748/wjg.v29.i36.5180

Figure 3 Graphical representation of liver metastases appearance on pre-contrast sequences and during the administration of hepatobiliary contrast agents. IP: In-phase imaging; OP: Out-of-phase imaging; DWI: Diffusion weighted imaging; T2WI: T2-weighted imaging; HBP: Hepatobiliary phase.

require any follow-up if identified in low-risk patients including patients with no known primary cancer, hepatic risk factors or hepatic failure[58,59].

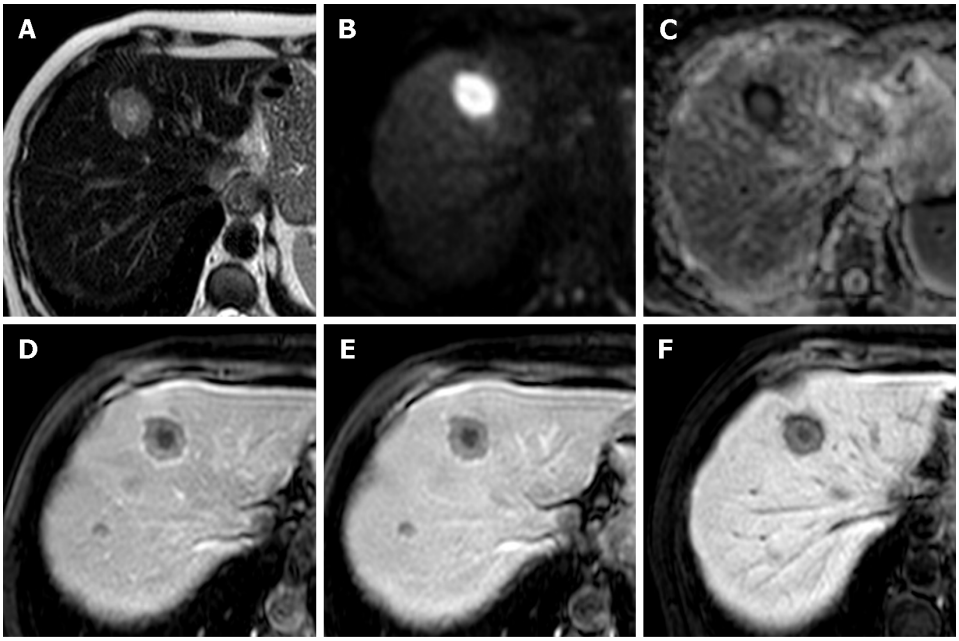

DOI: 10.3748/wjg.v29.i36.5180 **Copyright** ©The Author(s) 2023.

Figure 4 Liver metastases from colorectal cancer. A: EOB-magnetic resonance imaging of a 62-year-old woman demonstrates a liver lesion with hyperintensity on T2-weighted images; B: On diffusion weighted imaging the lesion appears markedly hyperintense; C: Apparent diffusion coefficient map demonstrates a peripheral hypointensity of the lesion; D: On the post-contrast arterial phase the lesion demonstrate reduced enhancement compared to the surrounding liver parenchyma with typical targetoid hypointensity; E: On the portal-venous phase the lesion remain hypovascular with targetoid appearance; F: On the hepatobiliary phase the lesion shows persistent hypoenhancement. Multiple other metastases were present in the liver parenchyma (not shown).

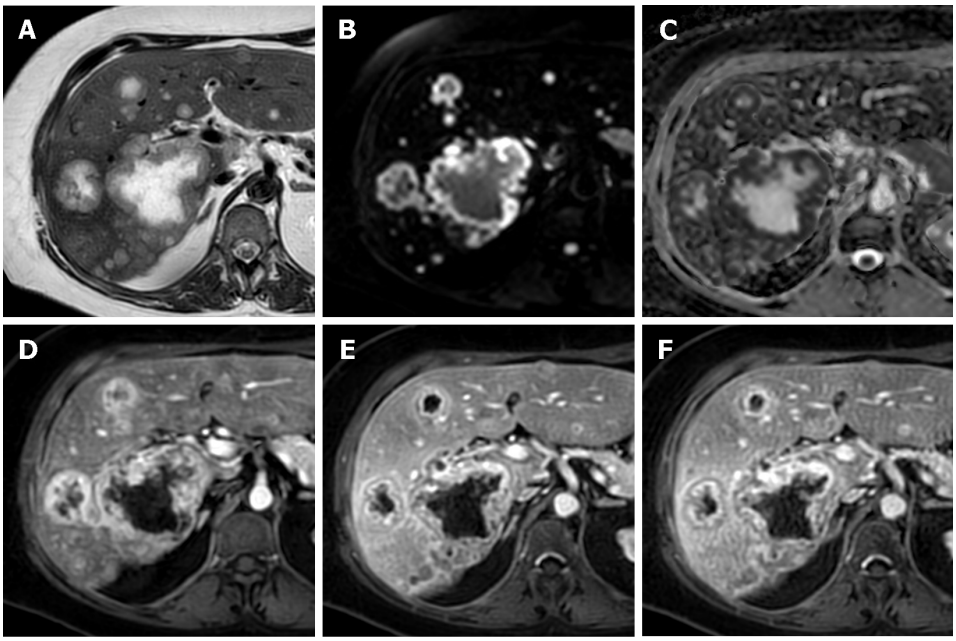

DOI: 10.3748/wjg.v29.i36.5180 **Copyright** ©The Author(s) 2023.

Figure 5 Multiple liver metastases from breast cancer. A: ECA-magnetic resonance imaging of a 51-year-old woman shows multiple liver lesions with central marker hyperintensity on T2-weighted images; B: Diffusion weighted imaging sequence demonstrates lesions' peripheral restricted diffusion; C: Apparent diffusion coefficient map shows a corresponding peripheral hypointensity of the lesions; D: On post-contrast arterial phase the lesions demonstrate a peripheral hyperenhancement rim with a central hypo-perfused area; E: On portal venous a corresponding peripheral washout is observed; F: On delayed post-contrast phase the peripheral hypoenhancement persists.

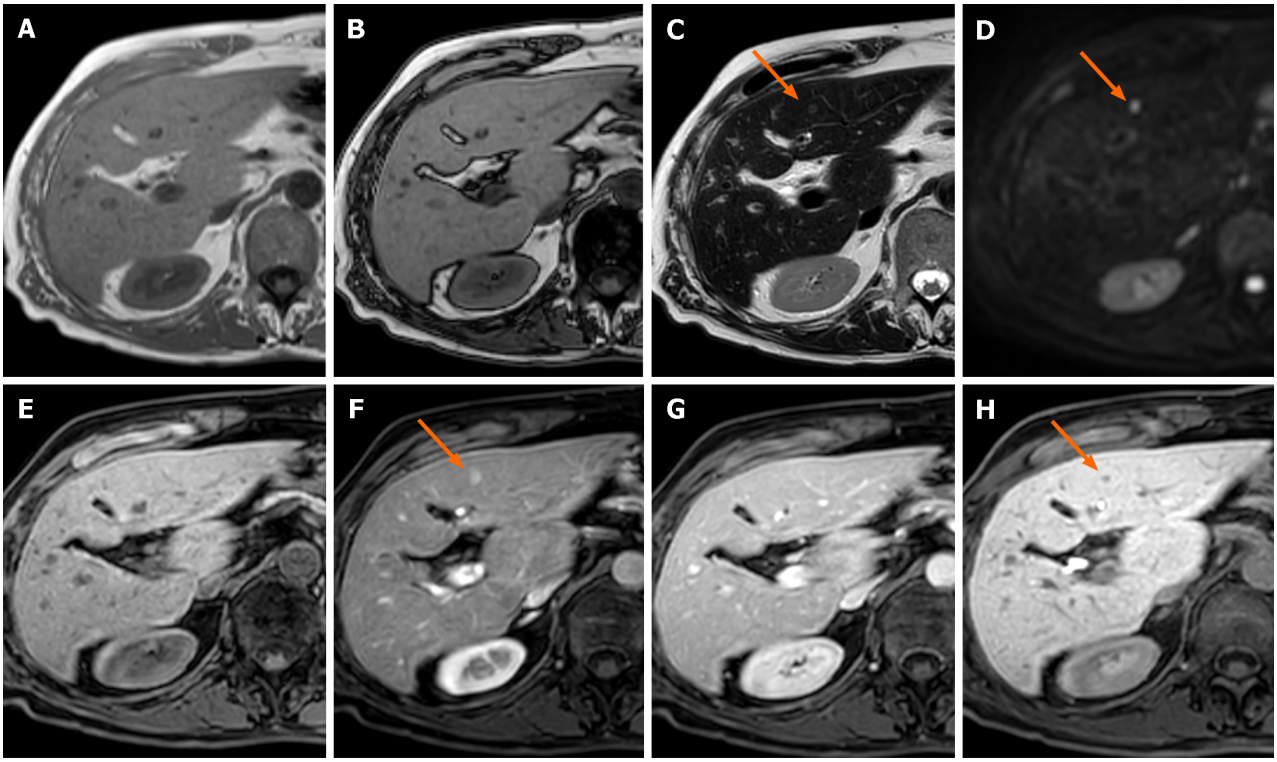

DOI: 10.3748/wjg.v29.i36.5180

Figure 6 Liver metastases from ileal neuroendocrine tumor. A: EOB-magnetic resonance imaging of a 55-year-old female patient shows a focal liver lesion isointense on in-phase images; B: On out-of-phase images, the lesions persist isointense compared to the healthy liver parenchyma; C: On T2-weighted images the lesion appears slightly hyperintense (orange arrow); D: Diffusion weighted imaging reveal restriction of diffusion of the lesion (orange arrow); E: Before contrast administration the lesion is isointense; F: During the post-contrast late hepatic arterial phase the lesion appears hypervascular (orange arrow); G: The lesion is isointense on the portal-venous phase; H: On the hepatobiliary phase lesion's low signal intensity is observed (orange arrow).

Indications to MRI for TSTC: TSTC lesions up to 1 cm identified on CT need follow-up with MRI at 3-6 mo whenever identified in high-risk patients, including patients with known primary cancer with a propensity for liver diffusion, cirrhosis, and/or other hepatic risk factors[58,59].

Characterization with MRI of TSTC lesions between 1 and 1.5 cm is indicated whenever suspicious imaging features are present or if "flash-filling" imaging features are identified in high-risk patients[58,59]. Suspicion imaging features embrace blurred margins, heterogeneous density, nodularity or mural thickening, thick septa, intermediate-to-high attenuation on portal venous–phase acquisitions, and enhancement of at least 20 HU between precontrast and post-contract CT[59].

In addition to the previous settings, MRI characterization or follow-up should be considered[58]:

(1) If an incidental TSTC lesion smaller than 1 cm is newly detected on CT follow-up even in low-risk patients;

(2) If a small cystic lesion is encountered in patients with ovarian cancer or GISTs;

And (3) In case of small TSTC growing over time.

MRI characterization of TSTC: MRI with and without injection of contrast media is oftentimes regarded as the problem solver for the characterization of hepatic TSTC. To date, contrast-enhanced MRI allows to permit a conclusive diagnosis in 95% of liver lesions, with only 1.5% of patients with MRIs requiring further exams[60]. The MRI diagnostic accuracy depends on the sequences acquired and type of contrast agent used, as well as the lesion itself. A step-by-step approach to MRI is mandatory for the characterization of hepatic TSTC. Non-contrast enhanced MRI sequences allow to identify some key imaging clues for the diagnosis of small benign lesions that should be regarded before looking at contrast-enhanced images. The analysis of T2W images and DWI are oftentimes sufficient to characterize small liver cysts and small hemangiomas which are the most common incidental liver lesions; indeed, both lesions will show a lack of diffusion restriction or the so-called "T2-shine through" phenomenon, and then cysts will be as bright as the cerebrospinal fluid on T2W sequences while hemangiomas will show a slightly lower hyperintensity as compared to the cerebrospinal fluid on T2W images[61]. A clear knowledge of these pre-contrast characteristics allows to avoid misdiagnosis if a "pseudo-washout" is identified on the 3-min phase with Gd-EOB-DTPA[62]. Dual-phase sequence, with in- and opposed-phase images, may allow to identify focal fat accumulation or focal fat sparing that may occasionally mimic a true liver lesion[63]. MRI without intravenous contrast agent may therefore answer the clinical question between benignity and malignancy in some cases. In addition, as Moosavi *et al*[64] demonstrated in their study on newly discovered indeterminate focal liver lesions in non-cirrhotic subjects, the information obtained from the HBP does not necessarily modify the diagnosis or the diagnostic confidence. Therefore, in selected cases if the radiologist is confident with the lesion characterization on non-contrast sequences (*e.g.* cyst, hemangioma), the routine use of intravenous contrast agent

may not be necessary[65]. Some TSTC lesions remain indeterminate after the assessment of non-contrast MRI sequences. In these cases, post-contrast images may prove to be helpful, and the choice of the contrast agent should be tailored on a per-patient and per-lesion bases. Contrast-enhanced MRI with ECAs may be particularly helpful if the slow-filling hemangioma is the most likely diagnosis and the acquisition of pure extracellular phases would allow to capture complete filling of the lesion. On the other hand, Gd-BOPTA MRI allows to obtain both pure delayed extracellular phases and HBP images although requiring acquisition at 2 h from contrast agent injection, and may be helpful if obtaining information from both delayed extracellular and HBP is deemed necessary. Finally, Gd-EOB-DTPA MRI allows to obtain an HBP at 10-20 min from contrast agent injection. For the differentiation between hepatocellular adenoma and FNH, the acquisition of the HBP may be very helpful in the majority of cases demonstrating iso-to-hyperintensity or a donut-like appearance on HBP in case of FNH and hypointensity on HBP in most cases of hepatocellular adenomas[66]. However, hepatocellular adenomas may occasionally demonstrate inhomogeneous iso-to-hyperintensity on HBP, thus leaving the final diagnosis to pathology for confirmation[41].

USEFULNESS OF DWI

The most sensitive MRI sequences to detect liver metastases are DWI and HBP images. Diffusion restriction and HBP hypointensity are typical features of liver secondary lesions[67] (Figure 7).

DWI technical principles are based on the evaluation of water molecules' motion and is currently used in clinical practice to assess lesions and tissue properties[67,68]. Specifically, b-values are DWI-related parameters able to assess the degree of diffusion of a specific lesion or tissue[69].

Considering that water diffusion in highly cellular tumors is more restricted compared to healthy tissues, a higher b-value might null signals from healthy tissues, resulting in marked cancer-to-healthy tissue contrast, thus leading to lesion hyperintense signals[68,69]. The diagnostic values of high b-values have been investigated and reported in several tumors, including liver metastases[70]. An important meta-analysis reported 87.1% (95%CI, 83.2%-90.1%) sensitivity for DWI in liver metastases detection[33]. Moreover, different studies showed that DWI was more sensitive than T2W images for CRC liver metastases[71-73]. In particular, it has been underlined the essential role of DWI, despite the very low spatial resolution, in the detection of small (≤ 1 cm) lesions[74].

The second most important parameter obtained by DWI is the ADC map, which correlates with tissue cellularity, relying on the mono-exponential model[69]. ADC values can help not only to characterize lesions but also to predict prognosis. Two meta-analyses established that ADC values might contribute to response to chemotherapy evaluation and prediction in CRC liver metastases[75,76]. Specifically, Drewes *et al*[76] demonstrated that the pre-treatment mean ADC in responder group was lower compared to the non-responder group (1.15×10^{-3} *vs* 1.37×10^{-3} mm^2/s, respectively). Similarly, Sobeh *et al*[75] demonstrated that the most robust response predictor to therapy was a lower baseline ADC value with a pooled mean difference of -0.12×10^{-3} mm^2/s among responders and non-responders. To strengthen these data, a systematic review confirmed that ADC value might be a promising tool for response to chemotherapy prediction in CRC liver metastases[77].

Moreover, the assessment of ADC values might be useful for the earlier evaluation of chemotherapy response in comparison with the RECIST criteria[76,78].

Indeed, Cui *et al*[79] reported an prompt increase in ADC values (on day 3 or day 7 after chemo) in responding lesions, thus representing the change in tissue composition: This aspect may allow clinicians to prevent overtreatment, thus avoiding adverse effects[78].

However, the ADC map may not be a sufficient diagnostic imaging method itself but needs to be integrated with other MRI sequences[80].

To move forward, it's important to highlight that the ADC map relies on the mono-exponential model based on the Gaussian movement of water molecules. However, considering that tumor heterogeneity affects the non-Gaussian diffusion behavior, two new diffusion techniques, namely intravoxel incoherent motion (IVIM) and diffusion kurtosis imaging (DKI), were introduced[78].

IVIM evaluates both diffusion and microcapillary perfusion modifications, analyzing the signal decay curve obtained from multiple b-values[81], while DKI is a straightforward extension of DWI providing a sensible measure of tissue structure depending on a probability distribution function[69,82]. Both modalities were analyzed by different studies, with a special focus as a predictor tool for response to therapy. In particular, Zhang *et al*[83] demonstrated the possible role of IVIM and DKI in predicting response to therapy in CRC liver metastases: At baseline, lower D values on IVIM map and higher *K* values on DKI map were independently associated with a good response to chemotherapy.

However, in clinical practice, DWI sequences are sometimes affected by artifacts, especially due to motions (cardiac pulsations and peristaltic movements) or magnetic susceptibility (especially at the boundary surfaces)[84].

Different techniques were developed to avoid or at least reduce the amount of artifacts, firstly to increase reader's confidence for the final diagnosis. In fact in 2021, some Authors aimed to compare the clinical utility of single-shot EPI using different breathing schemes and readout-segmented EPI (RS-EPI). The Authors found out that RS-EPI has the higher SNR, suggesting it as an emerging technique to be applied in everyday clinical practice[85]. More details regarding the usefulness of advanced DWI techniques are out of the scope of the present review; more details can be found in the review by Saito *et al*[84].

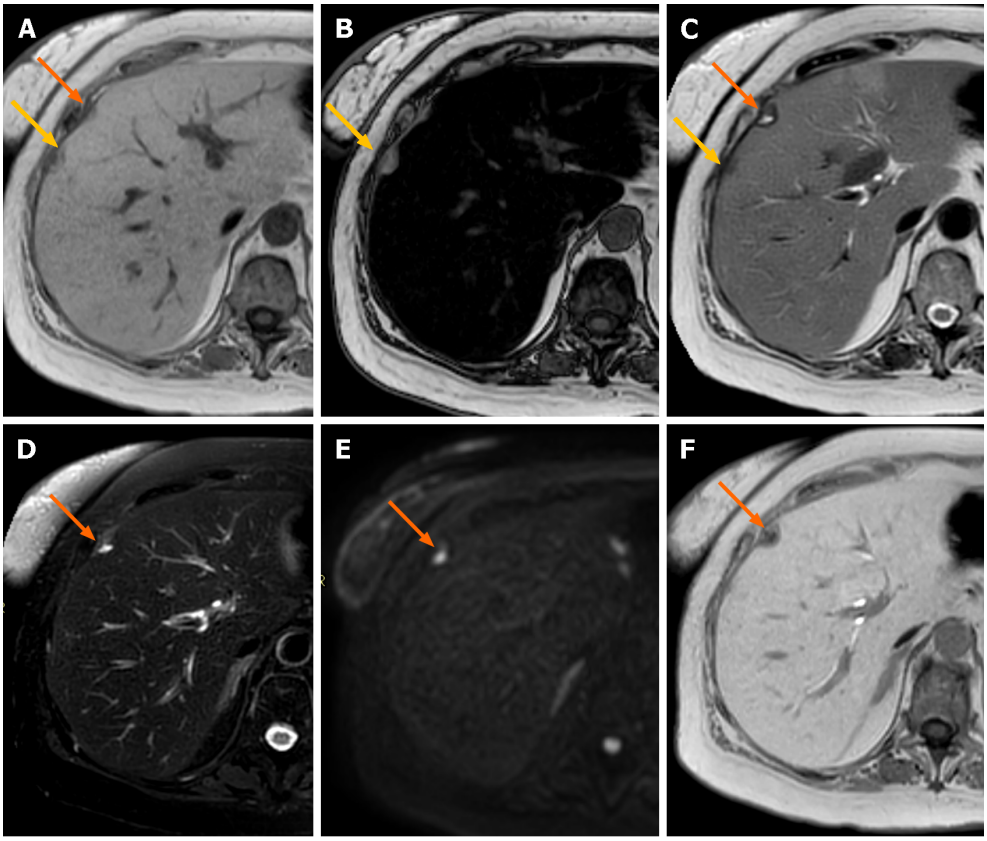

DOI: 10.3748/wjg.v29.i36.5180

Figure 7 Liver metastases from pancreatic adenocarcinoma. A: EOB-magnetic resonance imaging (MRI) of a 64-year-old woman shows two adjacent focal liver lesions (yellow and orange arrows) in the subcapsular region on the in-phase imaging; B: On out-phase imaging, one lesion (yellow arrow) shows hyperintensity, while the other one shows slight hypointensity. The liver is characterized by severe steatosis, considering the important signal drop-off between in-phase and out-of-phase imaging; C: On T2-weighted (T2W) imaging, one lesion (yellow arrow) is hypointense, while the other one (orange arrow) demonstrates inhomogeneous hyperintense signal; D: On fat-sat T2W sequence the low signal of the first lesion and the inhomogeneous high signal of the second one (orange arrow) are confirmed; E: Diffusion weighted imaging reveals focal restriction of diffusion corresponding to only one of the two lesions (orange arrow); F: On the hepatobiliary phase one lesion is isointense to liver parenchyma, while the second lesion shows a hypointense aspect. The final diagnosis for the lesion tagged by the orange arrow was liver metastasis from pancreatic adenocarcinoma, while the MRI characteristics of the lesion tagged by the yellow arrow are consistent with a focal fatty-sparing area.

THE ADDED VALUE OF GD-EOB-DTPA

Since its introduction, Gd-EOB-DTPA acquired a key role in characterization of malignant liver lesions, especially metastasis, and in evaluating response to therapy. One of the most important published randomized multicenter trials[86] demonstrated the superior diagnostic accuracy of Gd-EOB-DTPA, compared to ECAs-MRI and CT, in patients with suspected CRC liver metastases. The Authors demonstrated that no additional imaging was required for all patients who underwent EOB-MRI, while for patients who underwent ECA-MRI and CT further confirms were needed (in 17% and 39% of cases, respectively, $P < 0.0001$)[86].

An important systematic review and meta-analysis showed the higher per-lesion sensitivity of Gd-EOB-DTPA MRI in comparison to CT (median 94.9% *vs* 74.2%, respectively, $P < 0.001$). Higher diagnostic values of EOB-MRI were also demonstrated for small lesions (with an axial diameter < 1 cm), with a per-lesion sensitivity of 85.7% (*vs* 50%, $P < 0.001$) [87].

Vilgrain *et al*[33] published a meta-analysis regarding 1989 patients with 3854 Liver metastases to analyze diagnostic values of DWI and HPB acquired with Gd-EOB-DTPA alone and a combination of both. When considered singularly, HBP was more sensitive than DWI to detect liver metastases (90.6% *vs* 87.1%). However, the combination of both sequences showed the highest per-lesion sensitivity (95%, $P < 0.0001$).

Interestingly, Zech *et al*[88] evaluated the cost of the diagnostic workup of CRC liver metastases patients, three different imaging approaches were compared: EOB-MRI, ECA-MRI, and CT. Overall costs were lower when using Gd-EOB-DTPA as the first line imaging technique compared to different strategies. Indeed, no patient in the EOB-MRI group required supplementary imaging to decide on treatment as compared to 18.1% and 39.7% for patients who underwent ECAs-MRI and CT, respectively. To endorse these aspects, Renzulli *et al*[89] suggested that EOB-MRI should be the initial imaging modality of choice for patients pre-operatively evaluation.

Kim *et al*[90] studied the importance of EOB-MRI compared to CT in CRC patients with synchronous liver secondary lesions. They found out that EOB-MRI increased the detection of liver secondary lesions, helping a more fitted treatment,

with an overall increase in survival rate (estimated 5-year survival of 70.8% for EOB-MRI *vs* 48.1% for CT).

EOB-MRI has also proved useful for predicting therapeutic responses. Recently, Gu *et al*[91] evaluated whether some HBP parameters, such as the relative tumor enhancement (RTE) and the standard deviation value of signal intensity ratio (SDR), can predict the pathological response to systemic therapy in CRC liver metastases. RTE and SDR values were significantly higher in the responder group in comparison with the non-responder one ($P < 0.001$).

Similarly, Murata *et al*[92] demonstrated that the mean pre-treatment RTE was significantly higher in responders in comparison with the non-responder group (37.2% ± 10.9% *vs* 17.9% ± 10.5%, $P = 0.0006$). Larger and prospective studies should aim to better evaluate the usefulness of EOB-MRI as a prognostic factor in patients with liver metastases.

Finally, EOB-MRI is even worthwhile in the assessment of chemotherapy-induced liver disease, as in the case of sinusoidal obstruction syndrome, especially during the early stages. The under-expression of OATP by centrilobular hepatocytes reflects the reticular hypointensity appearance on HBP which can be more easily detected than with conventional MRI sequences[89,93].

ADVANCED TOOLS: RADIOMICS AND ARTIFICIAL INTELLIGENCE

Radiomics, which uses artificial intelligence (AI) techniques to extract and analyze quantitative features from medical images, has been proven as an effective tool in medical imaging to improve detection and characterization of diseases in terms of diagnosis and prognosis. These algorithms can analyze image patterns, extract meaningful features, and make predictions based on the data, providing valuable insights to clinicians. Among different clinical applications, radiomics has been proposed by researchers to face different challenges regarding liver metastases, mostly using CT images. Different algorithms have been proposed for diagnosis, prediction of development of liver metastases, response to therapy, recurrence, and survival[94].

AI applied to CT images has shown excellent results in detecting liver metastases with a sensitivity of 93%[95] and in making differential diagnosis between liver metastases from other liver lesions, reaching an accuracy of 92%[96]. Moreover, some studies assessed the feasibility of using radiomics for response prediction to therapy at lesion level also demonstrating the superiority of radiomic features compared to the standard biomarkers, such as size and RECIST[97].

Despite CT being the diagnostic tool most often used during staging and follow-up, and consequently, the one for which it is easier to develop radiomics tools, MRI is the only technique that allows providing quantitative data to assess morphological and functional information useful for tumor characterization and prediction of response to treatment. Therefore, efforts have been made to correlate MRI-based radiomics data to clinical outcomes. Zhang *et al*[98] demonstrated that radiomics features derived from pre-treatment T2W images can correlate with response to chemotherapy, *e.g.*, responding lesions showed a lower angular second moment and higher variance (two homogeneity measures) compared to non-responding ones. Similarly, but using post-treatment MRI features, Reimer *et al*[99] demonstrated that higher kurtosis on arterial and portal-venous images and higher skewness in portal-venous phase could identify patients undergoing TARE with a progressive disease earlier compared to standard RECIST criteria. However, when radiomics features are combined into statistical classifiers, *e.g.*, in a multivariate analysis, predictive performances are boosted. For example, Granata *et al*[100] proven that combining some radiomics features obtained from T2W images into a statistical classifier, such as the KNN, allows predicting the tumor growth with an area under the curve (AUC) of 0.9 in the validation set. Han *et al*[101] developed a model to preoperatively identify Histopathological Growth Patterns of CRC liver metastases, analyzing the tumor-liver interface zone on MR, reaching an AUC of 0.91 in the cohort of internal validation.

Radiomics has also shown promising results on MRI in the diagnostic field of research, distinguishing different types of liver lesions, and differentiating secondary lesions from benign lesions and primary liver cancer[102]. Finally, an important objective that has been pursued with radiomics is the correlation between radiomics and genomics through an approach called radiogenomics. Using MR-based radiomics features, Granata *et al*[103] assessed the RAS mutation status, a robust prognostic and predictive biomarker among subjects undergoing liver CRC metastases resection. They performed a multivariate analysis using features extracted from MRI, obtaining an accuracy of 87.5% with 91.7% of sensitivity and 83.3% of specificity on an external validation cohort in predicting RAS mutational status. Despite these promising results, further studies should be conducted to face important challenges such as the instability of radiomic features among different devices and acquisition protocols, especially for MRI images, lack of fully automatic segmentation tools and user-friendly interfaces[104], and shortage of well-annotated multicenter datasets. The latter can be overcome by designing clinical trials enhancing the cooperation between institutions and collaborations between clinicians and medical imaging experts.

CONCLUSION

Liver metastases are the most common malignant hepatic tumors occurring in everyday clinical practice, particularly during MR examinations. MRI, thanks to its multiparametric approach, can help radiologists to correctly evaluate and characterize liver metastases, reaching a fitted approach for each patient. The wide spectrum of liver metastases should be well-known, especially in the case of atypical appearance. The usefulness of HBAs, especially Gd-EOB-DTPA, has been widely demonstrated in the international literature and should be adopted whenever a liver MRI in patients with known primary tumors is required. Finally, MRI diagnostic accuracy can reach high values, representing nowadays the non-invasive reference standard technique to stage, re-stage and evaluate the prognosis of cancer patients with secondary

liver involvement.

Future directions should be focused firstly on the usefulness of MR as a prognostic tool in patients with liver metastases. Moreover, the integration of AI techniques, especially machine and deep learning models, should be considered to identify liver metastases and to enhance radiologists' confidence in the final diagnosis.

FOOTNOTES

Author contributions: All Authors equally contributed to this paper with the conception and design of the study, literature review and analysis, drafting and critical revision, and editing; All authors gave final approval of the final version.

Conflict-of-interest statement: All the authors report no relevant conflicts of interest for this article.

Country/Territory of origin: Italy

ORCID number: Cesare Maino 0000-0002-5742-802X; Federica Vernuccio 0000-0003-0350-1794; Roberto Cannella 0000-0002-3808-0785; Francesco Cortese 0000-0002-2731-3766; Paolo Niccolò Franco 0000-0001-8280-3787; Clara Gaetani 0000-0001-9303-4397; Valentina Giannini 0000-0001-5052-8231; Riccardo Inchingolo 0000-0002-0253-5936; Davide Ippolito 0000-0003-3870-0371; Arianna Defeudis 0000-0002-1745-3044; Giulia Pilato 0009-0004-6265-2079; Davide Tore 0000-0002-5087-5740; Riccardo Faletti 0000-0002-8865-8637; Marco Gatti 0000-0001-8168-5280.

S-Editor: Li L
L-Editor: A
P-Editor: Chen YX

REFERENCES

1 **Namasivayam S**, Martin DR, Saini S. Imaging of liver metastases: MRI. *Cancer Imaging* 2007; **7**: 2-9 [PMID: 17293303 DOI: 10.1102/1470-7330.2007.0002]
2 **Centeno BA**. Pathology of liver metastases. *Cancer Control* 2006; **13**: 13-26 [PMID: 16508622 DOI: 10.1177/107327480601300103]
3 **Tsilimigras DI**, Brodt P, Clavien PA, Muschel RJ, D'Angelica MI, Endo I, Parks RW, Doyle M, de Santibañes E, Pawlik TM. Liver metastases. *Nat Rev Dis Primers* 2021; **7**: 27 [PMID: 33859205 DOI: 10.1038/s41572-021-00261-6]
4 **Alberts SR**, Wagman LD. Chemotherapy for colorectal cancer liver metastases. *Oncologist* 2008; **13**: 1063-1073 [PMID: 18838438 DOI: 10.1634/theoncologist.2008-0142]
5 **Imam K**, Bluemke DA. MR imaging in the evaluation of hepatic metastases. *Magn Reson Imaging Clin N Am* 2000; **8**: 741-756 [PMID: 11149677 DOI: 10.1016/S1064-9689(21)00641-3]
6 **Horn SR**, Stoltzfus KC, Lehrer EJ, Dawson LA, Tchelebi L, Gusani NJ, Sharma NK, Chen H, Trifiletti DM, Zaorsky NG. Epidemiology of liver metastases. *Cancer Epidemiol* 2020; **67**: 101760 [PMID: 32562887 DOI: 10.1016/j.canep.2020.101760]
7 **Zane KE**, Cloyd JM, Mumtaz KS, Wadhwa V, Makary MS. Metastatic disease to the liver: Locoregional therapy strategies and outcomes. *World J Clin Oncol* 2021; **12**: 725-745 [PMID: 34631439 DOI: 10.5306/wjco.v12.i9.725]
8 **Niekel MC**, Bipat S, Stoker J. Diagnostic imaging of colorectal liver metastases with CT, MR imaging, FDG PET, and/or FDG PET/CT: a meta-analysis of prospective studies including patients who have not previously undergone treatment. *Radiology* 2010; **257**: 674-684 [PMID: 20829538 DOI: 10.1148/radiol.10100729]
9 **Floriani I**, Torri V, Rulli E, Garavaglia D, Compagnoni A, Salvolini L, Giovagnoni A. Performance of imaging modalities in diagnosis of liver metastases from colorectal cancer: a systematic review and meta-analysis. *J Magn Reson Imaging* 2010; **31**: 19-31 [PMID: 20027569 DOI: 10.1002/jmri.22010]
10 **Baghdadi A**, Mirpour S, Ghadimi M, Motaghi M, Hazhirkarzar B, Pawlik TM, Kamel IR. Imaging of Colorectal Liver Metastasis. *J Gastrointest Surg* 2022; **26**: 245-257 [PMID: 34664191 DOI: 10.1007/s11605-021-05164-1]
11 **Karaosmanoglu AD**, Onur MR, Ozmen MN, Akata D, Karcaaltincaba M. Magnetic Resonance Imaging of Liver Metastasis. *Semin Ultrasound CT MR* 2016; **37**: 533-548 [PMID: 27986172 DOI: 10.1053/j.sult.2016.08.005]
12 **Koh DM**. Liver-specific contrast agents. *Cancer Imaging* 2012; **12**: 363-364 [PMID: 23023233 DOI: 10.1102/1470-7330.2012.9022]
13 **Fiorentini G**, Sarti D, Aliberti C, Carandina R, Mambrini A, Guadagni S. Multidisciplinary approach of colorectal cancer liver metastases. *World J Clin Oncol* 2017; **8**: 190-202 [PMID: 28638789 DOI: 10.5306/wjco.v8.i3.190]
14 **Chandarana H**, Feng L, Ream J, Wang A, Babb JS, Block KT, Sodickson DK, Otazo R. Respiratory Motion-Resolved Compressed Sensing Reconstruction of Free-Breathing Radial Acquisition for Dynamic Liver Magnetic Resonance Imaging. *Invest Radiol* 2015; **50**: 749-756 [PMID: 26146869 DOI: 10.1097/RLI.0000000000000179]
15 **Hood MN**, Ho VB, Smirniotopoulos JG, Szumowski J. Chemical shift: the artifact and clinical tool revisited. *Radiographics* 1999; **19**: 357-371 [PMID: 10194784 DOI: 10.1148/radiographics.19.2.g99mr07357]
16 **Agostini A**, Kircher MF, Do RK, Borgheresi A, Monti S, Giovagnoni A, Mannelli L. Magnetic Resonanance Imaging of the Liver (Including Biliary Contrast Agents)-Part 2: Protocols for Liver Magnetic Resonanance Imaging and Characterization of Common Focal Liver Lesions. *Semin Roentgenol* 2016; **51**: 317-333 [PMID: 27743568 DOI: 10.1053/j.ro.2016.05.016]

17 **Baliyan V**, Das CJ, Sharma R, Gupta AK. Diffusion weighted imaging: Technique and applications. *World J Radiol* 2016; **8**: 785-798 [PMID: 27721941 DOI: 10.4329/wjr.v8.i9.785]

18 **Qayyum A**. Diffusion-weighted imaging in the abdomen and pelvis: concepts and applications. *Radiographics* 2009; **29**: 1797-1810 [PMID: 19959522 DOI: 10.1148/rg.296095521]

19 **Frydrychowicz A**, Lubner MG, Brown JJ, Merkle EM, Nagle SK, Rofsky NM, Reeder SB. Hepatobiliary MR imaging with gadolinium-based contrast agents. *J Magn Reson Imaging* 2012; **35**: 492-511 [PMID: 22334493 DOI: 10.1002/jmri.22833]

20 **Qu J**, Han S, Zhang H, Liu H, Wang Z, Kamel IR, Berthold K, Dominik NM, Zhang J, Zhang S, Dong Y, Jiang L, Liu C, Li H. Arterial Phase with CAIPIRINHA-Dixon-TWIST (CDT)-Volume-Interpolated Breath-Hold Examination (VIBE) in Detecting Hepatic Metastases. *Transl Oncol* 2017; **10**: 46-53 [PMID: 27940372 DOI: 10.1016/j.tranon.2016.11.005]

21 **Okada M**, Wakayama T, Yada N, Hyodo T, Numata K, Kagawa Y, Nishiyama D, Miyakoshi K, Murakami T. Optimal flip angle of Gd-EOB-DTPA-enhanced MRI in patients with hepatocellular carcinoma and liver metastasis. *Abdom Imaging* 2014; **39**: 694-701 [PMID: 24562726 DOI: 10.1007/s00261-014-0096-y]

22 **Jhan SR**, Wu YY, Chang PY, Chai JW, Su TC. Comparison of ability of lesion detection of two MRI sequences of T2WI HASTE and T2WI BLADE for hepatocellular carcinoma. *Medicine (Baltimore)* 2023; **102**: e32890 [PMID: 36820556 DOI: 10.1097/MD.0000000000032890]

23 **Gandhi SN**, Brown MA, Wong JG, Aguirre DA, Sirlin CB. MR contrast agents for liver imaging: what, when, how. *Radiographics* 2006; **26**: 1621-1636 [PMID: 17102040 DOI: 10.1148/rg.266065014]

24 **Matos AP**, Velloni F, Ramalho M, AlObaidy M, Rajapaksha A, Semelka RC. Focal liver lesions: Practical magnetic resonance imaging approach. *World J Hepatol* 2015; **7**: 1987-2008 [PMID: 26261689 DOI: 10.4254/wjh.v7.i16.1987]

25 **Welle CL**, Guglielmo FF, Venkatesh SK. MRI of the liver: choosing the right contrast agent. *Abdom Radiol (NY)* 2020; **45**: 384-392 [PMID: 31392396 DOI: 10.1007/s00261-019-02162-5]

26 **Neri E**, Bali MA, Ba-Ssalamah A, Boraschi P, Brancatelli G, Alves FC, Grazioli L, Helmberger T, Lee JM, Manfredi R, Martì-Bonmatì L, Matos C, Merkle EM, Op De Beeck B, Schima W, Skehan S, Vilgrain V, Zech C, Bartolozzi C. ESGAR consensus statement on liver MR imaging and clinical use of liver-specific contrast agents. *Eur Radiol* 2016; **26**: 921-931 [PMID: 26194455 DOI: 10.1007/s00330-015-3900-3]

27 **Wang C**, Yuan XD, Wu N, Sun WR, Tian Y. Optimization of hepatobiliary phase imaging in gadoxetic acid-enhanced magnetic resonance imaging: a narrative review. *Quant Imaging Med Surg* 2023; **13**: 1972-1982 [PMID: 36915322 DOI: 10.21037/qims-22-916]

28 **Kalor A**, Girometti R, Maheshwari E, Kierans AS, Pugliesi RA, Buros C, Furlan A. Update on MR Contrast Agents for Liver Imaging: What to Use and When. *Radiol Clin North Am* 2022; **60**: 679-694 [PMID: 35989037 DOI: 10.1016/j.rcl.2022.04.005]

29 **Reimer P**, Schneider G, Schima W. Hepatobiliary contrast agents for contrast-enhanced MRI of the liver: properties, clinical development and applications. *Eur Radiol* 2004; **14**: 559-578 [PMID: 14986050 DOI: 10.1007/s00330-004-2236-1]

30 **Chen L**, Zhang J, Zhang L, Bao J, Liu C, Xia Y, Huang X, Wang J. Meta-analysis of gadoxetic acid disodium (Gd-EOB-DTPA)-enhanced magnetic resonance imaging for the detection of liver metastases. *PLoS One* 2012; **7**: e48681 [PMID: 23144927 DOI: 10.1371/journal.pone.0048681]

31 **Winder M**, Grabowska S, Hitnarowicz A, Barczyk-Gutkowska A, Gruszczyńska K, Steinhof-Radwańska K. The application of abbreviated MRI protocols in malignant liver lesions surveillance. *Eur J Radiol* 2023; **164**: 110840 [PMID: 37141846 DOI: 10.1016/j.ejrad.2023.110840]

32 **Ozaki K**, Higuchi S, Kimura H, Gabata T. Liver Metastases: Correlation between Imaging Features and Pathomolecular Environments. *Radiographics* 2022; **42**: 1994-2013 [PMID: 36149824 DOI: 10.1148/rg.220056]

33 **Vilgrain V**, Esvan M, Ronot M, Caumont-Prim A, Aubé C, Chatellier G. A meta-analysis of diffusion-weighted and gadoxetic acid-enhanced MR imaging for the detection of liver metastases. *Eur Radiol* 2016; **26**: 4595-4615 [PMID: 26883327 DOI: 10.1007/s00330-016-4250-5]

34 **Furlan A**, Marin D, Bae KT, Lagalla R, Agnello F, Bazzocchi M, Brancatelli G. Focal liver lesions hyperintense on T1-weighted magnetic resonance images. *Semin Ultrasound CT MR* 2009; **30**: 436-449 [PMID: 19842568 DOI: 10.1053/j.sult.2009.07.002]

35 **Costa AF**, Thipphavong S, Arnason T, Stueck AE, Clarke SE. Fat-Containing Liver Lesions on Imaging: Detection and Differential Diagnosis. *AJR Am J Roentgenol* 2018; **210**: 68-77 [PMID: 29064755 DOI: 10.2214/AJR.17.18136]

36 **Porrello G**, Cannella R, Randazzo A, Badalamenti G, Brancatelli G, Vernuccio F. CT and MR Imaging of Retroperitoneal Sarcomas: A Practical Guide for the Radiologist. *Cancers (Basel)* 2023; **15** [PMID: 37296946 DOI: 10.3390/cancers15112985]

37 **Paulatto L**, Dioguardi Burgio M, Sartoris R, Beaufrère A, Cauchy F, Paradis V, Vilgrain V, Ronot M. Colorectal liver metastases: radiopathological correlation. *Insights Imaging* 2020; **11**: 99 [PMID: 32844319 DOI: 10.1186/s13244-020-00904-4]

38 **Danet IM**, Semelka RC, Leonardou P, Braga L, Vaidean G, Woosley JT, Kanematsu M. Spectrum of MRI appearances of untreated metastases of the liver. *AJR Am J Roentgenol* 2003; **181**: 809-817 [PMID: 12933487 DOI: 10.2214/ajr.181.3.1810809]

39 **Dahlqvist Leinhard O**, Dahlström N, Kihlberg J, Sandström P, Brismar TB, Smedby O, Lundberg P. Quantifying differences in hepatic uptake of the liver specific contrast agents Gd-EOB-DTPA and Gd-BOPTA: a pilot study. *Eur Radiol* 2012; **22**: 642-653 [PMID: 21984449 DOI: 10.1007/s00330-011-2302-4]

40 **Hui CL**, Mautone M. Patterns of enhancement in the hepatobiliary phase of gadoxetic acid-enhanced MRI. *Br J Radiol* 2020; **93**: 20190989 [PMID: 32462892 DOI: 10.1259/bjr.20190989]

41 **Vernuccio F**, Gagliano DS, Cannella R, Ba-Ssalamah A, Tang A, Brancatelli G. Spectrum of liver lesions hyperintense on hepatobiliary phase: an approach by clinical setting. *Insights Imaging* 2021; **12**: 8 [PMID: 33432491 DOI: 10.1186/s13244-020-00928-w]

42 **Park SH**, Kim H, Kim EK, Choi DK, Chung YE, Kim MJ, Choi JY. Aberrant expression of OATP1B3 in colorectal cancer liver metastases and its clinical implication on gadoxetic acid-enhanced MRI. *Oncotarget* 2017; **8**: 71012-71023 [PMID: 29050339 DOI: 10.18632/oncotarget.20295]

43 **Choi SH**, Kim SY, Park SH, Kim KW, Lee JY, Lee SS, Lee MG. Diagnostic performance of CT, gadoxetate disodium-enhanced MRI, and PET/CT for the diagnosis of colorectal liver metastasis: Systematic review and meta-analysis. *J Magn Reson Imaging* 2018; **47**: 1237-1250 [PMID: 28901685 DOI: 10.1002/jmri.25852]

44 **Nakai H**, Arizono S, Isoda H, Togashi K. Imaging Characteristics of Liver Metastases Overlooked at Contrast-Enhanced CT. *AJR Am J Roentgenol* 2019; **212**: 782-787 [PMID: 30779660 DOI: 10.2214/AJR.18.20526]

45 **Cannella R**, Cunha GM, Catania R, Chupetlovska K, Borhani AA, Fowler KJ, Furlan A. Magnetic Resonance Imaging of Nonhepatocellular Malignancies in Chronic Liver Disease. *Magn Reson Imaging Clin N Am* 2021; **29**: 404-418 [PMID: 34243926 DOI: 10.1016/j.mric.2021.05.009]

46 **Ikram NS**, Yee J, Weinstein S, Yeh BM, Corvera CU, Monto A, Hope TA. Multiple arterial phase MRI of arterial hypervascular hepatic lesions: improved arterial phase capture and lesion enhancement. *Abdom Radiol (NY)* 2017; **42**: 870-876 [PMID: 27770162 DOI:

10.1007/s00261-016-0948-8]
47 **Hong S**, Choi SH, Hong SB, Kim SY, Lee SS. Clinical usefulness of multiple arterial-phase images in gadoxetate disodium-enhanced magnetic resonance imaging: a systematic review and meta-analysis. *Eur Radiol* 2022; **32**: 5413-5423 [PMID: 35192009 DOI: 10.1007/s00330-022-08620-x]
48 **Borhani AA**, Wiant A, Heller MT. Cystic hepatic lesions: a review and an algorithmic approach. *AJR Am J Roentgenol* 2014; **203**: 1192-1204 [PMID: 25415696 DOI: 10.2214/AJR.13.12386]
49 **Lee JE**, Kim SH, Lee S, Choi SY, Hwang JA, Woo SY. Differentiating metastatic mucinous colorectal adenocarcinomas from simple cysts of the liver using contrast-enhanced and diffusion-weighted MRI. *Br J Radiol* 2018; **91**: 20180303 [PMID: 30040437 DOI: 10.1259/bjr.20180303]
50 **Patnana M**, Menias CO, Pickhardt PJ, Elshikh M, Javadi S, Gaballah A, Shaaban AM, Korivi BR, Garg N, Elsayes KM. Liver Calcifications and Calcified Liver Masses: Pattern Recognition Approach on CT. *AJR Am J Roentgenol* 2018; **211**: 76-86 [PMID: 29667888 DOI: 10.2214/AJR.18.19704]
51 **Hale HL**, Husband JE, Gossios K, Norman AR, Cunningham D. CT of calcified liver metastases in colorectal carcinoma. *Clin Radiol* 1998; **53**: 735-741 [PMID: 9817090 DOI: 10.1016/s0009-9260(98)80315-2]
52 **Kim SJ**, Choi JA, Lee SH, Choi JY, Hong SH, Chung HW, Kang HS. Imaging findings of extrapulmonary metastases of osteosarcoma. *Clin Imaging* 2004; **28**: 291-300 [PMID: 15246481 DOI: 10.1016/S0899-7071(03)00206-7]
53 **Engel S**, Dockerty MB. Calcification and ossification in rectal malignant processes. *JAMA* 1962; **179**: 347-350 [PMID: 13890226 DOI: 10.1001/jama.1962.03050050037006]
54 **Miele AJ**, Edmonds HW. Calcified liver metastases: a specific roentgen diagnostic sign. *Radiology* 1963; **80**: 779-785 [PMID: 13935630 DOI: 10.1148/80.5.779]
55 **Zhou Y**, Zhang J, Dan Pu, Bi F, Chen Y, Liu J, Li Q, Gou H, Wu B, Qiu M. Tumor calcification as a prognostic factor in cetuximab plus chemotherapy-treated patients with metastatic colorectal cancer. *Anticancer Drugs* 2019; **30**: 195-200 [PMID: 30570508 DOI: 10.1097/CAD.0000000000000726]
56 **Nakayama T**, Yoshimitsu K, Irie H, Aibe H, Tajima T, Shinozaki K, Nishie A, Kakihara D, Honda H. Fat in liver metastasis from renal cell carcinoma detected by chemical shift MR imaging. *Abdom Imaging* 2003; **28**: 657-659 [PMID: 14628870 DOI: 10.1007/s00261-003-0001-6]
57 **Khalil HI**, Patterson SA, Panicek DM. Hepatic lesions deemed too small to characterize at CT: prevalence and importance in women with breast cancer. *Radiology* 2005; **235**: 872-878 [PMID: 15833992 DOI: 10.1148/radiol.2353041099]
58 **Bird JR**, Brahm GL, Fung C, Sebastian S, Kirkpatrick IDC. Recommendations for the Management of Incidental Hepatobiliary Findings in Adults: Endorsement and Adaptation of the 2017 and 2013 ACR Incidental Findings Committee White Papers by the Canadian Association of Radiologists Incidental Findings Working Group. *Can Assoc Radiol J* 2020; **71**: 437-447 [PMID: 32515993 DOI: 10.1177/0846537120928349]
59 **Gore RM**, Pickhardt PJ, Mortele KJ, Fishman EK, Horowitz JM, Fimmel CJ, Talamonti MS, Berland LL, Pandharipande PV. Management of Incidental Liver Lesions on CT: A White Paper of the ACR Incidental Findings Committee. *J Am Coll Radiol* 2017; **14**: 1429-1437 [PMID: 28927870 DOI: 10.1016/j.jacr.2017.07.018]
60 **Margolis NE**, Shaver CM, Rosenkrantz AB. Indeterminate liver and renal lesions: comparison of computed tomography and magnetic resonance imaging in providing a definitive diagnosis and impact on recommendations for additional imaging. *J Comput Assist Tomogr* 2013; **37**: 882-886 [PMID: 24270109 DOI: 10.1097/RCT.0b013e3182aace0d]
61 **Holzapfel K**, Bruegel M, Eiber M, Ganter C, Schuster T, Heinrich P, Rummeny EJ, Gaa J. Characterization of small (≤10 mm) focal liver lesions: value of respiratory-triggered echo-planar diffusion-weighted MR imaging. *Eur J Radiol* 2010; **76**: 89-95 [PMID: 19501995 DOI: 10.1016/j.ejrad.2009.05.014]
62 **Vernuccio F**, Bruno A, Costanzo V, Bartolotta TV, Vieni S, Midiri M, Salvaggio G, Brancatelli G. Comparison of the Enhancement Pattern of Hepatic Hemangioma on Magnetic Resonance Imaging Performed With Gd-EOB-DTPA Versus Gd-BOPTA. *Curr Probl Diagn Radiol* 2020; **49**: 398-403 [PMID: 31253462 DOI: 10.1067/j.cpradiol.2019.06.006]
63 **Dioguardi Burgio M**, Bruno O, Agnello F, Torrisi C, Vernuccio F, Cabibbo G, Soresi M, Petta S, Calamia M, Papia G, Gambino A, Ricceri V, Midiri M, Lagalla R, Brancatelli G. The cheating liver: imaging of focal steatosis and fatty sparing. *Expert Rev Gastroenterol Hepatol* 2016; **10**: 671-678 [PMID: 27027652 DOI: 10.1586/17474124.2016.1169919]
64 **Moosavi B**, Shenoy-Bhangle AS, Tsai LL, Reuf R, Mortele KJ. MRI characterization of focal liver lesions in non-cirrhotic patients: assessment of added value of gadoxetic acid-enhanced hepatobiliary phase imaging. *Insights Imaging* 2020; **11**: 101 [PMID: 32960337 DOI: 10.1186/s13244-020-00894-3]
65 **Chernyak V**, Horowitz JM, Kamel IR, Arif-Tiwari H, Bashir MR, Cash BD, Farrell J, Goldstein A, Grajo JR, Gupta S, Hindman NM, Kamaya A, McNamara MM, Porter KK, Solnes LB, Srivastava PK, Zaheer A, Carucci LR, Expert Panel on Gastrointestinal Imaging. ACR Appropriateness Criteria® Liver Lesion-Initial Characterization. *J Am Coll Radiol* 2020; **17**: S429-S446 [PMID: 33153555 DOI: 10.1016/j.jacr.2020.09.005]
66 **Zech CJ**, Grazioli L, Breuer J, Reiser MF, Schoenberg SO. Diagnostic performance and description of morphological features of focal nodular hyperplasia in Gd-EOB-DTPA-enhanced liver magnetic resonance imaging: results of a multicenter trial. *Invest Radiol* 2008; **43**: 504-511 [PMID: 18580333 DOI: 10.1097/RLI.0b013e3181705cd1]
67 **Ablefoni M**, Surup H, Ehrengut C, Schindler A, Seehofer D, Denecke T, Meyer HJ. Diagnostic Benefit of High b-Value Computed Diffusion-Weighted Imaging in Patients with Hepatic Metastasis. *J Clin Med* 2021; **10** [PMID: 34830572 DOI: 10.3390/jcm10225289]
68 **Hazhirkarzar B**, Khoshpouri P, Shaghaghi M, Ghasabeh MA, Pawlik TM, Kamel IR. Current state of the art imaging approaches for colorectal liver metastasis. *Hepatobiliary Surg Nutr* 2020; **9**: 35-48 [PMID: 32140477 DOI: 10.21037/hbsn.2019.05.11]
69 **Tang L**, Zhou XJ. Diffusion MRI of cancer: From low to high b-values. *J Magn Reson Imaging* 2019; **49**: 23-40 [PMID: 30311988 DOI: 10.1002/jmri.26293]
70 **Kele PG**, van der Jagt EJ. Diffusion weighted imaging in the liver. *World J Gastroenterol* 2010; **16**: 1567-1576 [PMID: 20355235 DOI: 10.3748/wjg.v16.i13.1567]
71 **Coenegrachts K**, Delanote J, Ter Beek L, Haspeslagh M, Bipat S, Stoker J, Van Kerkhove F, Steyaert L, Rigauts H, Casselman JW. Improved focal liver lesion detection: comparison of single-shot diffusion-weighted echoplanar and single-shot T2 weighted turbo spin echo techniques. *Br J Radiol* 2007; **80**: 524-531 [PMID: 17510250 DOI: 10.1259/bjr/33156643]
72 **Parikh T**, Drew SJ, Lee VS, Wong S, Hecht EM, Babb JS, Taouli B. Focal liver lesion detection and characterization with diffusion-weighted MR imaging: comparison with standard breath-hold T2W imaging. *Radiology* 2008; **246**: 812-822 [PMID: 18223123 DOI: 10.1148/radiol.2463070432]

73 **Bruegel M**, Rummeny EJ. Hepatic metastases: use of diffusion-weighted echo-planar imaging. *Abdom Imaging* 2010; **35**: 454-461 [PMID: 19471997 DOI: 10.1007/s00261-009-9541-8]

74 **Mainenti PP**, Romano F, Pizzuti L, Segreto S, Storto G, Mannelli L, Imbriaco M, Camera L, Maurea S. Non-invasive diagnostic imaging of colorectal liver metastases. *World J Radiol* 2015; **7**: 157-169 [PMID: 26217455 DOI: 10.4329/wjr.v7.i7.157]

75 **Sobeh T**, Inbar Y, Apter S, Soffer S, Anteby R, Kraus M, Konen E, Klang E. Diffusion-weighted MRI for predicting and assessing treatment response of liver metastases from CRC - A systematic review and meta-analysis. *Eur J Radiol* 2023; **163**: 110810 [PMID: 37075628 DOI: 10.1016/j.ejrad.2023.110810]

76 **Drewes R**, Pech M, Powerski M, Omari J, Heinze C, Damm R, Wienke A, Surov A. Apparent Diffusion Coefficient Can Predict Response to Chemotherapy of Liver Metastases in Colorectal Cancer. *Acad Radiol* 2021; **28** Suppl 1: S73-S80 [PMID: 33008734 DOI: 10.1016/j.acra.2020.09.006]

77 **Beckers RCJ**, Lambregts DMJ, Lahaye MJ, Rao SX, Kleinen K, Grootscholten C, Beets GL, Beets-Tan RGH, Maas M. Advanced imaging to predict response to chemotherapy in colorectal liver metastases - a systematic review. *HPB (Oxford)* 2018; **20**: 120-127 [PMID: 29196021 DOI: 10.1016/j.hpb.2017.10.013]

78 **Caruso M**, Stanzione A, Prinster A, Pizzuti LM, Brunetti A, Maurea S, Mainenti PP. Role of advanced imaging techniques in the evaluation of oncological therapies in patients with colorectal liver metastases. *World J Gastroenterol* 2023; **29**: 521-535 [PMID: 36688023 DOI: 10.3748/wjg.v29.i3.521]

79 **Cui Y**, Zhang XP, Sun YS, Tang L, Shen L. Apparent diffusion coefficient: potential imaging biomarker for prediction and early detection of response to chemotherapy in hepatic metastases. *Radiology* 2008; **248**: 894-900 [PMID: 18710982 DOI: 10.1148/radiol.2483071407]

80 **Nalaini F**, Shahbazi F, Mousavinezhad SM, Ansari A, Salehi M. Diagnostic accuracy of apparent diffusion coefficient (ADC) value in differentiating malignant from benign solid liver lesions: a systematic review and meta-analysis. *Br J Radiol* 2021; **94**: 20210059 [PMID: 34111960 DOI: 10.1259/bjr.20210059]

81 **Kim JH**, Joo I, Kim TY, Han SW, Kim YJ, Lee JM, Han JK. Diffusion-Related MRI Parameters for Assessing Early Treatment Response of Liver Metastases to Cytotoxic Therapy in Colorectal Cancer. *AJR Am J Roentgenol* 2016; **207**: W26-W32 [PMID: 27303858 DOI: 10.2214/AJR.15.15683]

82 **Jensen JH**, Helpern JA, Ramani A, Lu H, Kaczynski K. Diffusional kurtosis imaging: the quantification of non-gaussian water diffusion by means of magnetic resonance imaging. *Magn Reson Med* 2005; **53**: 1432-1440 [PMID: 15906300 DOI: 10.1002/mrm.20508]

83 **Zhang H**, Li W, Fu C, Grimm R, Chen Z, Zhang W, Qiu L, Wang C, Zhang X, Yue L, Hu X, Guo W, Tong T. Comparison of intravoxel incoherent motion imaging, diffusion kurtosis imaging, and conventional DWI in predicting the chemotherapeutic response of colorectal liver metastases. *Eur J Radiol* 2020; **130**: 109149 [PMID: 32659615 DOI: 10.1016/j.ejrad.2020.109149]

84 **Saito K**, Tajima Y, Harada TL. Diffusion-weighted imaging of the liver: Current applications. *World J Radiol* 2016; **8**: 857-867 [PMID: 27928467 DOI: 10.4329/wjr.v8.i11.857]

85 **Xie S**, Masokano IB, Liu W, Long X, Li G, Pei Y, Li W. Comparing the clinical utility of single-shot echo-planar imaging and readout-segmented echo-planar imaging in diffusion-weighted imaging of the liver at 3 tesla. *Eur J Radiol* 2021; **135**: 109472 [PMID: 33370640 DOI: 10.1016/j.ejrad.2020.109472]

86 **Zech CJ**, Korpraphong P, Huppertz A, Denecke T, Kim MJ, Tanomkiat W, Jonas E, Ba-Ssalamah A; VALUE study group. Randomized multicentre trial of gadoxetic acid-enhanced MRI versus conventional MRI or CT in the staging of colorectal cancer liver metastases. *Br J Surg* 2014; **101**: 613-621 [PMID: 24652690 DOI: 10.1002/bjs.9465]

87 **Vreugdenburg TD**, Ma N, Duncan JK, Riitano D, Cameron AL, Maddern GJ. Comparative diagnostic accuracy of hepatocyte-specific gadoxetic acid (Gd-EOB-DTPA) enhanced MR imaging and contrast enhanced CT for the detection of liver metastases: a systematic review and meta-analysis. *Int J Colorectal Dis* 2016; **31**: 1739-1749 [PMID: 27682648 DOI: 10.1007/s00384-016-2664-9]

88 **Zech CJ**, Justo N, Lang A, Ba-Ssalamah A, Kim MJ, Rinde H, Jonas E. Cost evaluation of gadoxetic acid-enhanced magnetic resonance imaging in the diagnosis of colorectal-cancer metastasis in the liver: Results from the VALUE Trial. *Eur Radiol* 2016; **26**: 4121-4130 [PMID: 26905871 DOI: 10.1007/s00330-016-4271-0]

89 **Renzulli M**, Clemente A, Ierardi AM, Pettinari I, Tovoli F, Brocchi S, Peta G, Cappabianca S, Carrafiello G, Golfieri R. Imaging of Colorectal Liver Metastases: New Developments and Pending Issues. *Cancers (Basel)* 2020; **12** [PMID: 31936319 DOI: 10.3390/cancers12010151]

90 **Kim C**, Kim SY, Kim MJ, Yoon YS, Kim CW, Lee JH, Kim KP, Lee SS, Park SH, Lee MG. Clinical impact of preoperative liver MRI in the evaluation of synchronous liver metastasis of colon cancer. *Eur Radiol* 2018; **28**: 4234-4242 [PMID: 29691635 DOI: 10.1007/s00330-018-5422-2]

91 **Gu XL**, Cui Y, Wang K, Xing Q, Li XT, Zhu HT, Li ZW, Sun YS. Qualitative and quantitative parameters on hepatobiliary phase of gadoxetic acid-enhanced MR imaging for predicting pathological response to preoperative systemic therapy in colorectal liver metastases. *Eur J Radiol* 2022; **157**: 110572 [PMID: 36327859 DOI: 10.1016/j.ejrad.2022.110572]

92 **Murata S**, Matsushima S, Sato Y, Yamaura H, Kato M, Hasegawa T, Muro K, Inaba Y. Predicting chemotherapeutic response for colorectal liver metastases using relative tumor enhancement of gadoxetic acid disodium-enhanced magnetic resonance imaging. *Abdom Radiol (NY)* 2018; **43**: 3301-3306 [PMID: 29666951 DOI: 10.1007/s00261-018-1615-z]

93 **Yoneda N**, Matsui O, Ikeno H, Inoue D, Yoshida K, Kitao A, Kozaka K, Kobayashi S, Gabata T, Ikeda H, Nakamura K, Ohta T. Correlation between Gd-EOB-DTPA-enhanced MR imaging findings and OATP1B3 expression in chemotherapy-associated sinusoidal obstruction syndrome. *Abdom Imaging* 2015; **40**: 3099-3103 [PMID: 26187715 DOI: 10.1007/s00261-015-0503-z]

94 **Rompianesi G**, Pegoraro F, Ceresa CD, Montalti R, Troisi RI. Artificial intelligence in the diagnosis and management of colorectal cancer liver metastases. *World J Gastroenterol* 2022; **28**: 108-122 [PMID: 35125822 DOI: 10.3748/wjg.v28.i1.108]

95 **Hamm CA**, Wang CJ, Savic LJ, Ferrante M, Schobert I, Schlachter T, Lin M, Duncan JS, Weinreb JC, Chapiro J, Letzen B. Deep learning for liver tumor diagnosis part I: development of a convolutional neural network classifier for multi-phasic MRI. *Eur Radiol* 2019; **29**: 3338-3347 [PMID: 31016442 DOI: 10.1007/s00330-019-06205-9]

96 **Liu Y**, Kohlberger T, Norouzi M, Dahl GE, Smith JL, Mohtashamian A, Olson N, Peng LH, Hipp JD, Stumpe MC. Artificial Intelligence-Based Breast Cancer Nodal Metastasis Detection: Insights Into the Black Box for Pathologists. *Arch Pathol Lab Med* 2019; **143**: 859-868 [PMID: 30295070 DOI: 10.5858/arpa.2018-0147-OA]

97 **Rao SX**, Lambregts DM, Schnerr RS, Beckers RC, Maas M, Albarello F, Riedl RG, Dejong CH, Martens MH, Heijnen LA, Backes WH, Beets GL, Zeng MS, Beets-Tan RG. CT texture analysis in colorectal liver metastases: A better way than size and volume measurements to assess response to chemotherapy? *United European Gastroenterol J* 2016; **4**: 257-263 [PMID: 27087955 DOI: 10.1177/2050640615601603]

98 **Zhang H**, Li W, Hu F, Sun Y, Hu T, Tong T. MR texture analysis: potential imaging biomarker for predicting the chemotherapeutic response

of patients with colorectal liver metastases. *Abdom Radiol (NY)* 2019; **44**: 65-71 [PMID: 29967982 DOI: 10.1007/s00261-018-1682-1]

99 **Reimer RP**, Reimer P, Mahnken AH. Assessment of Therapy Response to Transarterial Radioembolization for Liver Metastases by Means of Post-treatment MRI-Based Texture Analysis. *Cardiovasc Intervent Radiol* 2018; **41**: 1545-1556 [PMID: 29881933 DOI: 10.1007/s00270-018-2004-2]

100 **Granata V**, Fusco R, De Muzio F, Cutolo C, Setola SV, Grassi R, Grassi F, Ottaiano A, Nasti G, Tatangelo F, Pilone V, Miele V, Brunese MC, Izzo F, Petrillo A. Radiomics textural features by MR imaging to assess clinical outcomes following liver resection in colorectal liver metastases. *Radiol Med* 2022; **127**: 461-470 [PMID: 35347583 DOI: 10.1007/s11547-022-01477-6]

101 **Han Y**, Chai F, Wei J, Yue Y, Cheng J, Gu D, Zhang Y, Tong T, Sheng W, Hong N, Ye Y, Wang Y, Tian J. Identification of Predominant Histopathological Growth Patterns of Colorectal Liver Metastasis by Multi-Habitat and Multi-Sequence Based Radiomics Analysis. *Front Oncol* 2020; **10**: 1363 [PMID: 32923388 DOI: 10.3389/fonc.2020.01363]

102 **Jansen MJA**, Kuijf HJ, Veldhuis WB, Wessels FJ, Viergever MA, Pluim JPW. Automatic classification of focal liver lesions based on MRI and risk factors. *PLoS One* 2019; **14**: e0217053 [PMID: 31095624 DOI: 10.1371/journal.pone.0217053]

103 **Granata V**, Fusco R, Avallone A, De Stefano A, Ottaiano A, Sbordone C, Brunese L, Izzo F, Petrillo A. Radiomics-Derived Data by Contrast Enhanced Magnetic Resonance in RAS Mutations Detection in Colorectal Liver Metastases. *Cancers (Basel)* 2021; **13** [PMID: 33504085 DOI: 10.3390/cancers13030453]

104 **Fiz F**, Viganò L, Gennaro N, Costa G, La Bella L, Boichuk A, Cavinato L, Sollini M, Politi LS, Chiti A, Torzilli G. Radiomics of Liver Metastases: A Systematic Review. *Cancers (Basel)* 2020; **12** [PMID: 33036490 DOI: 10.3390/cancers12102881]

Published by **Baishideng Publishing Group Inc**
7041 Koll Center Parkway, Suite 160, Pleasanton, CA 94566, USA
Telephone: +1-925-3991568
E-mail: bpgoffice@wjgnet.com
Help Desk: https://www.f6publishing.com/helpdesk
https://www.wjgnet.com